Response to review 1

We thank the reviewer for their comments. Each comment is addressed below with the original review in italics, our responses in normal font and changes to the manuscript in bold.

In this manuscript, the authors describe and evaluate the land and ocean carbon cycle components coupled to the ACCESS-ESM1 model. For the land model, they focus on comparing the significance of having prognostic versus prescribed LAI values. The former is found to produce higher temporal variability in globally averaged GPP and respiration. They show that biases in the vegetation carbon simulated in the model is related to the physical model that supplies insufficient precipitation in certain regions. The evaluation of the ocean carbon cycle is done through comparing ACCESS-ESM1 to a subset of CMIP5 models and with observations, focusing on the surface tracers and carbon flux and NPP processes. Following a 1000 yrs of preindustrial run, the WOMBAT is a source of carbon to the atmosphere, and the authors attribute this to the bias in the surface alkalinity.

The study fits well within the scope of GMD, but it is my opinion that the manuscript is too brief with many missing elements essential for a carbon cycle model evaluation manuscript. The introduction should be extended to elaborate better the motivations and justifications for the need of such documentation. As it is, it is unclear if the purpose is simply to produce a technical description of the model or to evaluate the model performance, or both. Below I have some general comments and suggestions to improve the manuscript, followed by more specific comments.

The aim of the paper was to provide both a technical description of the model and, alongside the companion paper (Ziehn et al.), to evaluate the model. We apologise for the delay in submitting the Ziehn et al. manuscript and understand that the delay has made the review of this paper more difficult. Ziehn et al. has been submitted so that it should be available, at least on GMDD, by the time this paper is finalised. The final paragraph of the introduction will be divided into two (**now three**) paragraphs with the **second (and third**) paragraph providing more clarity on the scope of this paper (in respect to both the model description and evaluation) and that of the Ziehn et al companion paper. In particular section references will be included. **Rewritten introduction, particularly p4, line 16 – p5, line 8.**

General comments: The authors often refer to an accompanying paper by Ziehn et al.,which appears to analyze the same model for historical simulation. Given the limited evaluation that can be done for the preindustrial simulation, it may be worthwhile to combine them into one study. Otherwise, both papers should be submitted and available at the same time in GMDD for the reviewers. For instance, on page 8079, lines 6-7, the reader is referred to a different publication for information regarding impact on the atmospheric CO2. I found this difficult to comprehend since this impact on atm. CO2 should be seen in the preindustrial simulation as well. At the least, the authors have to provide some statements summarizing the finding in Ziehn et al. whether or not the impact is significant, why, etc..

It is our hope that both papers will be available together as soon as possible, as part 1 and 2 of the same study. While there are many ways that the model evaluation could have been divided across the two papers, we generally tried to match the simulation period with the period of observations. Thus, for land carbon especially, most of the comparison with observations is limited to present-day conditions and hence the historical simulation in the Ziehn et al. paper. Evaluation of the pre-industrial simulation focussed on aspects of the simulation that require many simulation years such as equilibration and interannual to decadal variability. We will try to make this clearer in the introduction (**a re-written final paragraph, p4-5**) and in the first paragraph of Section 4. **(p15, line 5-18)**

The motivation for evaluating the current model against ACCESS1.3 on page 8079 is also unclear. Why not compare against observations? If there is a strong motivation to understand the improvement in

the physical model, than this needs to be stated up front. In this case, more details on the physical improvements should be provided in the model description section. Are these improvements expected and why? As it is, section 4.1 and Fig. 2 appear to be unnecessary and disconnected from the rest of the manuscript. Consider to add more details in the simulated bias or improvement in the spatial precipitation pattern here as the authors pointed out that precipitation bias in the model leads to bias in land vegetation.

Since many components of the model had been previously documented, our focus here was on noting the updates/differences from those previously published versions. This was particularly true for the physical climate model. It was well documented in the ACCESS1.3 version and hence our aim was to show only that the physical model (ACCESS1.4) underlying our ESM (Carbon-cycle) version performed closely enough to ACCESS1.3 that the earlier documentation was still valid for the current model version. In effect, no or little improvement was expected between ACCESS1.3 and ACCESS1.4 and that was the purpose of Fig 2, to confirm that the performance was very similar. Since this has obviously caused some confusion, we propose to move the description of the ACCESS1.4 differences from ACCESS1.3 to an appendix. This will ensure the model evolution is captured while allowing the body of the paper to focus more explicitly on ACCESS-ESM1 including relevant aspects of its physical climate simulation. **Section 4.1, p15, now focusses on the climate impact of the two land carbon configurations, with ACCESS1.3/ACCESS1.4 differences moved to Appendix A, p33-34.**

For the ocean evaluation, we now show key diagnostics of the ACCESS-ESM simulation (meridional overturning, mixed layer depth, sea-ice) and directly assess them and compare them to other CMIP5 simulations. The assessment is now focused on ACCESS-ESM. We do include a short summary paragraph on how ACCESS-ESM and its simulation differs from previously published ACCESS results. **(Fig 3, Fig 4, p16-17)**

For the Ocean physics, page 8081, the first paragraph essentially can be summarized into the last sentence, which makes the paragraph appear unnecessary. But I think there are many details being left out here. E.g., why lower AABW strength lead to warmer deep ocean? Why MLD in the two simulations differ in the Ross and Weddell Seas? Is there any new physical parameterization that would lead to this differences? How these changes impact the distribution of biogeochemical tracers (see also additional comment below).}

We just present the ACCESS-ESM results and then compare it to both CMIP5 simulations and ACCESS1.3. We then follow this with a more thorough discussion of some of the key differences between ACCESS-ESM and ACCESS1.3 in regards to AAWB and MLD **(p16, line 23-p17, line 4)**. Some discussion of the consequences for BGC will be provided later in the paper when we assess the ocean BGC.**(Sec 4.3.3, p26-p28)**

For the land model, the comparison between prescribed vs prognostic LAI is certainly interesting, but there is also limited actual evaluation for its performance compare observational estimates or other CMIP5 models (some suggestions are provided in the specific comments below).

When ESMs are run in concentration-driven mode, it is generally assumed that simulating the carbon cycle has no impact on the climate simulation. We chose to present both prescribed and prognostic LAI cases here to note the climate impact of using prognostic LAI as well as to demonstrate the changed variability in land carbon fluxes with prognostic LAI. These impacts can be assessed in a pre-industrial simulation. For comparisons with observations and other CMIP5 models, this is more easily done for present-day conditions and hence is covered by Ziehn et al. (for GPP, LAI, carbon pool size etc). **Introduction now notes the reason for running prescribed and prognostic LAI cases, p4, line 26-28 and why comparison with present-day observations is in Ziehn et al., p5, line 5-7.**

There are many hand-waving statements throughout the manuscript, which can relatively easy to confirm with more detailed assessments. For example, it is stated in the abstract (and P8089) that the "model overestimates surface nitrate values", but this is based on the relative difference in the globally averaged values between model and observations (WOA). And the authors attribute this bias to the export of particulate organic carbon (POC). How so? The model computes nitrate based on stoichiometric ratio to phosphate, with no explicit nitrogen cycle and nitrogen fixation, so it is not directly obvious that this bias is due to POC. A spatial surface nitrate map compare to the WOA and its difference would be more helpful in identifying the mechanism responsible for the bias. Is there similar bias with phosphate? Other source of bias could also be attributed to the parameterization of the ecosystem model (e.g., phytoplankton growth, zooplankton grazing rates, etc.), circulation, etc.

First, we have dropped all references to nitrate because, as formulated, the model limiting macro nutrient is phosphate. Hence any link to processes like nitrogen fixation and denitrification are not relevant. Second, we now discuss the potential causes of the biases in the surface phosphate and link them to processes like phosphate uptake, POM remineralization and ocean circulation. To do this we have added figures of NPP, surface phosphate, Export Production (through 100m), and air-sea CO_2 fluxes **(Fig 14)**. The figure shows both the ocean-only forced simulation and the subsequent coupled simulation. Most of the problems with the NPP appear in the coupled simulation, which reflects changes in the tropical circulation in the coupled model. The problem is most apparent in NPP because of excessive recycling of phosphate in the photic zone. Interestingly, by the time one gets to CO_2 fluxes the differences between the ocean only and the coupled model are much less (**p26, line 15 – p27, line 27**).

P8081, end of last paragraph: The authors indicate and later state that the bias in the freshwater fluxes leads to bias in alkalinity, pCO2, and finally air-sea CO2 fluxes. Again, this statement is not confirmed by the quantitative analysis available in the manuscript. Wouldn't alkalinity bias due to freshwater fluxes, be cancelled out by the respective DIC-bias? I think how the model formulate the inorganic carbon formation in the surface and fluxes throughout the water column also plays a major role and should be tested before the above statement can be made.

It is better stated as biases in the salinity, which reflects both freshwater fluxes and the ocean circulation.
Yes, you are correct that bias in the alkalinity fields are partially linked to the export of calcium carbonate from the photic zone. By including a figure of the zonally averaged alkalinity section it is clear that the present simulation overestimates calcium carbonate export and underestimates the vertical gradient of alkalinity **(Fig 15)**. However, the salinity biases are also important because of the high correlation between salinity and alkalinity in the ocean (both observed and modelled). While both DIC and ALK are influenced by the freshwater flux the former tracer can flux out at the surface while the latter one cannot. Therefore low salinity at the surface is also associated with low alkalinity and both biases help to explain the positive trend in the sea-air flux of CO_2.
We have modified the text to say salinity biases are important to alkalinity and given the correlation of Sea surface salinity (SSS) with the observations we would not expect or want alkalinity to represent the data much better than SSS **(p25, line 11-20)**. While alkalinity does contain the biases that exist in the SSS simulation, further investigation shows the vertical alkalinity gradient is too strong and alkalinity is too low in the upper ocean implying we should reduce the calcium carbonate export too. (**p28, line 7-9**)

For the ocean carbon cycle performance, the authors focus on the surface sea-air carbon fluxes and NPP. There is no discussions on the interior biogeochemistry. Given that the paper evaluates the deep water ventilation (Section 4.1), it is necessary to also discuss how large scale ocean circulation

(together with vertical particle fluxes and remineralization) alter the biogeochemical tracers distribution in the interior ocean. If parallel BGC simulations with different physical are not available, some assessment on the tracer budgets within the available long simulations would be useful to assess the stability of the model. Mean state of vertical section in different basin compare to observation can also be helpful.

Following the reviewers request we have added an assessment of the interior BGC fields by comparing the zonally averaged sections of DIC, ALK, oxygen and Phosphate with observations **(Fig 15, and text p27-28)**. We have also added time series plots of the global averaged DIC, ALK and sediment DIC and ALK values so the reader can assess the model drift (**Fig 11, and text p23-24**). Note the sediment pool of DIC and ALK is small because the sediments are remineralized back into the water column on the annual timescale. This prevents large pools accumulating in the sediments but was done to improve numerical stability, by preventing instantaneous remineralization in the bottom in shallow water causing a large change in the BGC tracers.

The DIC in the ocean is slowly equilibrating with the atmosphere and if we expand the plot of the global net air-sea flux one can see a declining trend in the flux, which will require many thousands of years to reach a net flux of zero. Complicating the trend to a zero net flux is a climate system that is also not equilibrated and is also drifting to its mean state. **(Fig 11 now focussed on final 100 years of simulation)**

Specific and technical comments: Page 8073, Line 28: How is the partial pressure of CO2 computed? Briefly describe the inorganic carbon chemistry formulation used.
Following the OCMIP3 protocol pCO_2 ocean is computed using the simulated T, S, PO_4, DIC and Alk. (**p9, line 26-27**)

P8074, L21: consider replacing 'increasing' with 'changing'
Done. **(p10, line 18)**

P8074, L24: remove 'responding to'
Done. **(p10, line 20)**

P8075, L15: What is the spatial resolution of the land? Vertical resolution of the ocean?
Land resolution information will be added in the first paragraph of Section 3 and the second paragraph of Sec 3.1.1 (variable number of vegetation types per grid-cell). The ocean vertical resolution will be added at the end of the first paragraph of Section 3. (**p11, line 10-11, p11, line 14-15)**

P8075, L26: Describe the values of the `observed land carbon uptake'. Which data set? Global or regional? To my knowledge, there is no directly observed land carbon uptake.
This sentence has been modified to note that it is estimated global land carbon uptake and the data sources are given in the Zhang et al., 2014 paper. **(p12, line 4)**

P8076, L26: CMIP5 historical and RCP scenarios
Done. **(p13, line 3)**

P8077, L23: It is not clear if the fertilizer application here represents anthropogenic ornot. I would assume this is natural because of the preindustrial period. Please clarify.

This is anthropogenic fertiliser despite being for the preindustrial period, because the same set-up is also used for the historical and future periods. The set-up is a compromise between using present-day

fertiliser application rates but only applying them to the pre-industrial crop area. The last sentence of Section 3.1.1 has been rewritten to make this clearer. **(p13, line 29 – p14, line 2)**

P8080, L15-16: Add a brief statement and reference to why we expect such small impact?
'confirms' in this sentence was confusing. It was meant to indicate that an impact was expected, for the reasons stated on p8076, line 7-8, but given the size of the impact was uncertain, 'confirms' was misleading. We propose to change 'confirms' to 'indicates' and allow the paragraph following to elaborate on the difference and the link between the LAI and temperature change. **Sentence deleted in rewrite of Sec 4.1 and shift of material to appendix.**

P8080, last paragraph: For non specialist readers, it would be useful to include some statements describing how LAI relates or impacts surface temperature.
We have added in this paragraph an example of how the LAI could impact albedo for a snow-covered surface. We have also added a counter example where a large change in LAI has the opposite impact to a small change in LAI, and now note that there is no simple relationship between LAI and temperature since changes in LAI can potentially change many components of the surface energy balance. **(p15, line 27- p16, line 7)**

P8081, L3: 500 year control, but Fig 14 shows 1000 years model run. Are these two different runs? Would be useful to provide a table list of all performed simulations.
This paragraph will be rewritten as ACCESS-ESM1 results will now be shown rather than those from ACCESS1.4. ACCESS1.3-ACCESS1.4 differences will be noted in an appendix. This will reduce the number of model simulations referred to in the body of the manuscript and hence we do not feel that a table of simulations is necessary. **(Appendix A, p31)**

P8082, L6: 601-700. Why not years 901-1000?
The conservation check was performed before the model simulation had completed. There is no evidence that conservation behaviour has changed significantly over the final centuries of the simulation. This is now noted in the first sentence of Section 4.2.1. **(p17, line 17)**

P8082, L12: Why choose this number: "2gC/m2"? Is there observational evidence to suggest this as indicative of a steady state? Some explanation/references would be useful.
As noted in the text, the distribution of imbalances was highly skewed with most tiles close to zero and a small proportion of tiles with much larger positive imbalances (up to ~11000 gC/m2/100y in the ProgLAI case). Given all negative imbalances were small (minimum value -1.88 gC/m2/100y in the ProgLAI case), we took this as indicative of the precision of the carbon balance calculation and thus assumed that ±2gC/m2/100y indicated carbon conservation within the precision of the calculation. We have modified the first two paragraphs of Section 4.2.1 to explain this choice. **(p17, line 20-26)**

P8082, L21-23: This statement needs to be better supported by additional, relatively straight forward, analysis. For instance, is it possible to find other regions with similar LAI/PFT characteristic (to this region) but with contrasting precipitation pattern? If so, do they show the expected plant growth?
The paragraph has been rewritten to include information from an example transect across India. This example shows that the size of the leaf carbon pool for the crop pft is highly correlated with the amount of rainfall. This supports the statement that plant growth is limited by rainfall. **(p18, line 8-13)**

Section 4.2.1: What are the budgets of the land carbon pools (vegetation/soil/litter/etc.)? How do they compare spatially with observational estimates or other CMIP5 models (Lifeng et al., 2015; Todd-Brown et al., 2013, and references therein).

The carbon pools are compared with observations and other CMIP5 models in Ziehn et al. as it is more appropriate to do this from the historical simulation. Overall ACCESS-ESM1 gives pool sizes that agree reasonably well with observations.

P8084, L2-3: "Early test simulations ...getting too low,..." More explanation is needed here. What mechanism causes the nitrogen drift? How strong is the drift?
The issue was with the choice of initial pool sizes, which were too far out of balance to allow a sensible equilibrium to be reached. This was resolved by not allowing the inorganic soil mineral nitrogen and soil labile phosphorus pools to go below a minimum value of 0.5 gNm^{-2} and 0.1 gPm^{-2} respectively. Effectively a small source of nitrogen and phosphorus is input to the system predominantly through the model spin-up phase. The frequency with which this fix is required was assessed by checking how many tiles were at the minimum value at different parts of the simulation. Tundra and deciduous needleleaf vegetation types are the most affected vegetation types and more so for phosphorus than nitrogen, with the fraction of affected tiles dropping from over 40-60% to less than 5% for phosphorus and from 11-14% to less than 8% for nitrogen (nitrogen was incorrectly highlighted in the manuscript but this will be fixed and a more accurate description of the problem will be included). **(p19, line 23-25)**

While clarifying this issue, we found an error in eq 5 in the paper which should include multiplication by 'c' which effectively acts as a tuning parameter. This has been fixed and the values of the extra parameter have been added to the supplementary table. **(Now equation 3, p7, line 23)**

P8084, L12-14: Cite reference for this statement.
This statement was describing features seen in the figure. We have changed the sentence from 'There is a suggestion of ...' to 'The figure shows ...' to make this clearer. (**p20, line 4-5)**

P8084, last paragraph: please add some statements describing why the nitrogen and phosphorus pools behave differently? Some illustrative time series would be useful.
Nitrogen and phophorus timeseries have been added to Figure 6 (as panels c and d) and the description in the text will be expanded to address the 'why' question. **(Fig 6c, 6d, p20, line 15-16)**

P8085, 1st paragraph: How this spatial pattern compares to other CMIP5 models and observational estimates (e.g., Fluxnet, Jung et al., 2011)?
The seasonal cycle and spatial distribution of GPP are compared with observations and CMIP5 models in Ziehn et al., Sec 5.1.1.

P8085, L19-22: I consider this as one of the key findings of this study and should be highlighted more in the abstract or elaborated better in the conclusions as how to remedy this caveat.
The response of vegetation, particularly the C4 vegetation type, to low rainfall is now mentioned in the conclusions along with a potential new development which may improve this aspect of the simulation. **(p30, line1-4)**

P8086, L7-24: It is not clear what is the purpose of assessing the inter-annual variability (IAV) of the simulated GPP, NEE, etc. Is it critical for specific climate/carbon cycle projection? This motivation can be added into the introduction section. Is there observational evidence that support the simulated IAV?
Understanding the sensitivity of land carbon fluxes to climate on interannual timescales can aid in understanding how these fluxes may respond to externally forced climate change, and models can be more easily validated on interannual timescales (e.g. Fig 6.17, Ciais et al., WG1 AR5 Chapter 6, 2013). Observational evidence to support the simulated IAV is only available for the present day but we will check its comparability to our pre-industrial simulation. **Sentence added to introduction, p5, line 1-3; p22, line 22-27)**

P8087, L19-22: What are the differences? Is it possible to assess the reason behind these differences?
The ocean-only simulation has quite different dynamics to the coupled simulation which has implications for the biogeochemistry and the ability to use ocean-only simulations to help with the spin-up. This will be addressed more explicitly in our revisions including some figures from an ocean only simulation. **(p23, line 17-19, Fig 14, Sec 4.3.3)**

P8088, L2-3: This statement would be better supported with figures showing time series of DIC budget at different depth intervals (surface, intermediate depth, interior,...).
Figures will be added to show the time-series of interior DIC at different depths to provide information on the evolution of DIC. **(Fig 11)**

P8088, L4-5: How does the simulated spatial pattern compare to observation, consideradd maps of NPP and its difference with the observation.
The spatial distribution of NPP will be added to the paper, both for the ACCESS-ESM1 simulation and for an ocean-only case. **(Fig 14, Sec 4.3.3)**

P8090, L16-17: Consider adding a similar figure as Fig 7 for sea-air CO2 fluxes together with observations.
It is not possible to directly compare to observations since the observation include both the natural and anthropogenic fluxes. But we now show the simulated fluxes and the observed values to enable some comparison of them **(Fig 14)**. Regional and seasonal sea-air CO_2 fluxes are compared with observations in Ziehn et al.

P8092, L2: reducing surface salinity biases
Done **(p30, line 5)**

Figs 3 and 4 captions: why not show results from ACCESS-ESM1 model (instead of ACCESS1.4) to be consistent with the title of the paper?
We now only show ACCESS-ESM and then discuss how it compares to other CMIP models and to previous ACCESS versions. **(Fig 3, 4 and captions update, p48-49)**

Fig 7b: Very difficult to distinguish the green lines. Why are there two solid green lines on certain latitudes? For the 'all other types' (solid thin green lines), are these relevant for your discussions? If not, I suggest to remove these lines to make the figure clearer, or use different colors.
There are two bold green lines at some latitudes because there are two types of evergreen trees: broadleaf and needleleaf. The figure has been redrawn to distinguish these two types. All other types are shown as thin solid lines to demonstrate the statements in the text that in the tropics all the vegetation types have lower prognostic LAI than the prescribed LAI, while in the northern mid-latitudes the opposite is true; all vegetation types give larger prognostic LAI than prescribed. We feel this is an important point to make, but it does not require each vegetation type to be identified in the figure, and hence we prefer to leave the thin green lines unchanged. **(Revised Fig 7, p52)**

Fig 11a: Why are there some discontinuities in the time series?
As discussed in the methods section there were instabilities in the DIC tracer which we remedy by a slight change in the numerics of the ocean BGC equations. The instability causes the fluxes to go off-scale and then slowly recover. We now show this behaviour rather than mask the anomalous fluxes.
(Fig 11 now focusses on years 900-1000 during which time the discontinuity does not occur)

Fig 14: Consider replacing the colormap for the top panel with that used in Fig 13
Done (**Fig 14d, p59**)

Response to review 2

We thank the reviewer for their comments. Each comment is addressed below with the original review in italics, our responses in normal font and changes to the manuscript in bold.

This is an important study describing the behavior of the Australian Community Climate and Earth System Simulator (ACCESS) for pre-industrial simulations of the coupled global carbon climate system. The paper is well suited for publication in GMD however there are a number of short comings to the paper in the current form. The main concern is in the assessment of the CABLE land carbon simulations. While the paper contains a long history of the development of the CABLE model with many references to the various versions of the model and input files, the comparisons between the model versions provides no assessment of the simulated carbon cycle against other models or against observations.

This paper was always intended to be part 1 of a two part study. Unfortunately delays in getting part 2 (Ziehn et al.) submitted have made this paper more difficult to assess and we apologise for this. Part 2 presents the historical simulation for this model and particularly for the land carbon, part 2 is where we compare against observations and other models. We have rewritten the introduction (**especially the final paragraphs, p4, line 16 – p5, line 8**) and the first paragraphs of section 4 **(p14-15)** to try and be clearer about the scope of this paper, noting that aspects of the ocean carbon can be more easily assessed against observations from a pre-industrial simulation while comparisons of land carbon against observations are easier under present-day conditions. Part 2 has now been submitted and will hopefully be available online shortly.

The lack of systematic model evaluation results in a limited framework for the reader to assess the usefulness of the model for historical or projected future climate carbon simulations.

We have aimed to provide complementary analysis across part 1 and part 2 of the study and have chosen to focus in part 1 on the equilibration of land carbon fluxes and pools and on variability. The sensitivity of the model to interannual variations in temperature and precipitation may be useful in understanding how the model responds to future changes in temperature or precipitation. We will make that link clearer in our revised manuscript (**p5, line 1-3**). We will also check the comparability of our pre-industrial carbon sensitivity to temperature and precipitation with that seen in present-day observations and models (e.g. Fig 6.16, Ciais et al., WG1 AR5 Chapter 6, 2013). **(p22, line 22-28)**

The description and evaluation contain unnecessary detail in some areas such as page 8 lines 1 to 16.

The page 8 description is part of documenting changes between CABLE1.8 and CABLE2.2.3 in the context of ACCESS1.3 to ACCESS1.4 model differences. While this detail is useful for providing a link back to the ACCESS1.3 published model version we agree it is a distraction from the main ACCESS-ESM description and hence propose to move this material to an appendix. (**p32)**

The climate assessment of the various versions of ACCESS on page 17 is particularly complex and uninformative. It requires the reader to assess a range of unknown models against each other without any observations to assess model bias and variability.

The aim was to demonstrate that there was little difference in our physical climate model simulation from the previously published ACCESS1.3. We agree that the figure was complex and propose to move it to the appendix, **(p34)** replacing it in the main text with a figure focussed around the difference in land temperature between our two ACCESS-ESM1 configurations and how both relate to observations. (**new Fig 2, p15-16)**

For the ocean, assessment of the physical climate will now focus on ACCESS-ESM1 rather than ACCESS1.4 and on fields that are most relevant to carbon. **(p16-17)**

The land carbon assessment comparing the prescribed LAI version of the model against the prognostic carbon model investigates the relative differences in the terrestrial carbon cycle of the models but misses more fundamental metrics. In the introduction the authors refer to two important studies for assessing land carbon simulations and their fluxes to the atmosphere (Anav et al. 2013 and Shao et al. 2013). The paper could be greatly improved by simplifying the model description and the carbon cycle evaluation using the framework and metrics found in these papers. This would provide much needed objective assessment of the ACCESS model against other earth system models and global estimates of the terrestrial carbon cycle.

Our part 2 paper (Ziehn et al) contains many similar assessments to Anav et al and Shao et al, since those assessments rely on model simulations of the present day period. In particular Ziehn et al plot the seasonality of regional GPP and LAI similar to Fig 9 and Fig 11 of Anav et al, and provide timeseries of land temperature and precipitation comparable to Fig 1 and 2 of Anav et al. Global total carbon fluxes are compared with other models based on the data presented in Shao et al, Fig 2 and carbon pools are assessed against the analysis in Todd-Brown et al., (Biogeosciences, 10, 1717-1736, 2013). We have not attempted to reproduce the summary metrics presented in Fig 18-21 in Anav et al., because they would be time consuming to reproduce (being relative across models) and we do not believe they would add significantly to our model assessment.

In many parts of the paper the authors digress into thought experiments about the lack of carbon conservation or unusual behavior in the model but provide no metrics or statistical relationships to support these hypotheses.

As noted by the other reviewers, the lack of carbon conservation is important to understand and explain. We will describe an example transect which illustrates the relationship between rainfall and low leaf carbon (**p18, line 8-13**). We also now note how the mismatch between leaf carbon pool and LAI leads to issues with the relative magnitude of simulated GPP and leaf respiration **(p18, line 19-20)**. The limited regional extent of the carbon conservation problems will be noted, and the impact on NEE will be illustrated through a supplementary figure (**p19, line 13-16)**.

Therefore in order for this paper to be ready for publication I would recommend the authors simplify the model description down to the relevant information and then provide a systematic assessment of the carbon cycle model against other CMIP5 models and global carbon cycle estimates.

A restructure of the paper to move less relevant model description and assessment to the appendix should help improve the relevance of the main text. For ocean carbon, comparison with other CMIP5 models and global carbon cycle estimates is appropriate for this paper describing the pre-industrial simulation while for land carbon, these comparisons are best undertaken for the historical simulation and hence are presented in the second part of this study (Ziehn et al.).

Response to review 3

We thank the reviewer for their comments. Each comment is addressed below with the original review in italics, our responses in normal font and changes to the manuscript are in bold.

This paper describes the coupled Earth System Model (ESM) ACCESS-ESM1, integrating components for the atmosphere, land, sea ice, and the ocean. The innovation that goes into the model presented here is the coupling of carbon (C) cycle models on land and in the ocean, that (potentially) interact with climate. These climate-carbon cycle feedbacks arise due to the fact that all C (CO2) exchange fluxes between reservoirs on land and in the ocean are sensitive to climate and because climate itself is sensitive to atmospheric CO2, affected by these exchange fluxes. Tremendous amounts of work goes into the development of each of these components, and the coupling of these components itself is a major step forward and and will provide a highly desired addition to the relatively small ensemble of ESMs available already today. The components integrated into ACCESS-ESM1 themselves are not new and are used in other ESM in different constellations. Hence, the characteristics of the ESM presented here should not deviate substantially from other ESM predictions. Nevertheless, developing a new coupled model setup is all but trivial, it's like taking the training-wheels off the uncoupled components, and the coupled system should satisfy a set of key checks and benchmarks.

'Taking off the training wheels' is a good analogy. There can be unanticipated consequences when running the coupled system, even under prescribed atmospheric CO_2, and we felt it was important that these be documented. Our challenges with land carbon conservation had not been encountered in standalone simulations run with observed meteorology. Likewise, there has been a noticeable degradation of some aspects of our ocean carbon climatology compared to an ocean only simulation (which we will show more explicitly in our revised paper, **Fig 14**). The choice we made to focus our land carbon analysis on prescribed vs prognostic LAI was, in a sense, taking one training wheel off at a time. It might be assumed in a prescribed atmospheric CO_2 simulation that the carbon cycle has no impact on the climate simulation. We wanted to test that assumption by comparing the prescribed LAI case which has no climate interaction with the prognostic LAI case where some modification to climate occurs. **(Choice now noted in introduction, p4, line26-28)** When computing resources are limited, this is useful information for determining if we need to run both climate-only and earth-system model versions in the future.

Considering the size of the type of models presented here (in terms of number of processes represented, amount of code, computational resources required, etc.), a comprehensive description of such a model is impossible and model testing is a major task that can fill a books. From the perspective of a reviewer, it is thus impossible to really judge on the science that goes into this model, let alone to reproduce results (although GMD requires open-access and the possibility for reviewers to replicate results). Nevertheless, an transparent overview should be provided and key tests and benchmarks should be satisfied. As noted by the authors, this model should be used for future model intercomparison projects, like CMIP6, and the present paper should demonstrate that the model is up to this task.

We agree that it has been a challenging task to provide sufficient model description and evaluation to adequately document the model. For this reason we chose to split our model evaluation across 'Part 1' and 'Part 2' papers, focussing on the pre-industrial and historical period respectively. We apologise that delays in getting Part 2 submitted may have made this paper more difficult to assess.

First, I would like to define the challenge better. What does a coupled ESM model have to satisfy and be able to predict? The setup chosen here is to simulate the coupled Earth System, with a focus on climate, ocean circulation, and the C cycle, under constant preindustrial conditions. Given this, the system should equilibrate, i.e. gross C exchange fluxes between atmosphere, ocean, and land may persist, but

the net fluxes should attain zero (no model drift). However, a non-zero net flux e.g. into ocean sediments may persist over longer time scales. It has to be acknowledged that limiting computational resources may inhibit a perfect equilibration, this is common also for other ESMs. But even more crucially, mass should be conserved within the system. E.g., the total amount of C present in ocean, plus atmosphere, plus land should be constant.

We deliberately chose this 'simplest' case (**reasoning now noted p4, line 23-25**) to present here in order to document how our model behaved in respect of carbon conservation and equilibration, alongside describing our carbon climatology. We agree that C conservation and equilibration to zero are important tests but they are not necessarily easy to ensure in the coupled system. **Justification for concentration-driven cases now given in introduction, p3, line 13-22.**

I have major concerns about whether the ACCESS-ESM1 is ready for publication regarding these aspects. Both equilibration and mass conservation are not satisfied here, as the authors note on several occasions. Even after 1000 yr, land still emits 0.4 PgC/yr (ProgLAI case). Similarly, the ocean outgassing after 1000 yr is 0.6 PgC/yr. This is on the order of one fourth of the present-day global net flux in from these respective reservoirs.

Actually the land emission is only 0.14 PgC/yr in the ProgLAI case (but 0.4 PgC/yr in the PresLAI case). As we note in the manuscript, the non-zero land emission is largely accounted for (0.33 out of 0.40 PgC/y for PresLAI, 0.09 out of 0.14 PgC/y for ProgLAI) by tiles that are non-conserving. These are restricted to relatively small geographical regions (Figure 1) (**now noted p19, line 13-16**), in India and in eastern tropical South America (and wetland tiles for PresLAI). This figure will be made available as **supplementary information**. In a prescribed atmospheric CO_2 simulation, as used here, land carbon fluxes are diagnostic only, and have no impact on the simulation of carbon fluxes from any other location. Hence there is no reason for the simulation as a whole to be significantly degraded by these regional errors. It is also worth noting that even if carbon had been conserved in these regions, the low rainfall available to support plant growth would still result in the gross carbon fluxes tending towards zero as in our current work. Thus these regions are unlikely to provide good estimates of land carbon fluxes, in part due to rainfall biases in the physical model over which we have no direct control.

The net air-sea flux is slowly decreasing as shown by the expanded plot of the last 100 years of the simulation (Figure 2). To reach steady-state will take many thousand of years. The large bias in the simulation reflects the low surface alkalinity of the ocean model, which is partially attributed to a low surface salinity (a common feature of coupled models, see Fig 12: Taylor diagram in the paper) and to excessive export of calcium carbonate. While we could increase the surface alkalinity to make the net flux nearly zero the model will continue to drift. Note the magnitude of the outgassing is comparable to other CMIP5 simulations of the pre-industrial. **(Fig 11 has been modified to focus on the final 100 years of the simulation and Sec 4.3.1, p23 now contains further discussion of the slow equilibration).**

The other major concerns I have is whether the model is even tested for what it is supposed to provide. Coupled ESMs are used to quantify climate-carbon cycle feedbacks and predict atmospheric CO2 under future CO2 emission (and climate) trajectories. This is a notable difference to providing climate projections given atmospheric CO2. A coupled model should be able, after equilibration and under constant boundary conditions (radiative forcing from other agents, solar radiation), to simulate constant atmospheric CO2 concentrations, with gross exchange fluxes between the atmosphere land and ocean (GPP on land and in the ocean) being broadly consistent with observations. This is not tested here. Atmospheric CO2 concentrations are prescribed in both simulations. I argue that this is not a sufficient setup for a test of a coupled ESM.

Coupled ESMs are being routinely used (e.g. CMIP5) in both concentration-driven and emissions-driven configurations, the former focussed towards the diagnosis of carbon fluxes and the latter to carbon-climate feedbacks. Both uses are valid and we will now note this in our introduction (**p3, line 13-22**). The analysis presented here of the simpler concentration-driven case has shown that our model would not perform realistically in an emissions-driven configuration without the application of a carbon flux correction. We will make this clear in the conclusions of our paper **(p30, line 11-13)**. The inability of the ACCESS-ESM1 model to perform emissions-driven simulations without carbon flux correction, does not negate the model being useful for carbon flux diagnosis in concentration-driven cases across historical and future periods. For this reason, documentation of ACCESS-ESM1 in its current form remains important.

I acknowledge that a balance has to be found between depth and conciseness in the assessment that can be handled under limited resources and published as a GMD paper. I also acknowledge that such a model development is always work-in-progress but should still be publishable. However, I am not convinced that the work in progress presented here has yet reached a state from where it can be taken further (e.g., by adding complexity, as noted by the authors).

We will rewrite our conclusions to be clearer about what the model is suitable for in its current form, what needs to be improved to allow for a wider range of studies and where we are limited by our underlying physical model. We agree that there is little value in adding complexity to the model until we have dealt with some of the more basic issues that this study has uncovered. **(Conclusions rewritten, p28-31)**

*I am listing a set of variables/aspects that may be addressed by a coupled model under constant boundary conditions and assessed *by comparison agains observations*. This is a suggestion for a next round of review. Some of these are already addressed (e.g. meridional overturning) but in many instances only as a comparison to a previous model version is given and not to observations.*

We acknowledge that our manuscript was potentially confusing because different comparisons were made for different parts of the simulation: the physical climate was compared to a previous model version, land carbon was compared between two different ACCESS-ESM1 configurations while ocean carbon was compared with observations and other CMIP5 models. In our revised manuscript we will be clearer about the scope of this paper and that of Part 2; Ziehn et al. (where land carbon is assessed against observations and other CMIP5 models) (**rewritten final paragraphs of introduction, p4, line 16 – p5, line 8**). We will also move material related to different versions of the physical model (ACCESS1.3/ACCESS1.4) to an **appendix (p31-34)** so that the main body of the text is focussed more clearly on ACCESS-ESM1. For the ocean, we have added a number of additional figures (as suggested) to enable a better assessment of the simulation by comparing to observations (**Fig 4, extra panels Fig 11, Fig 14, Fig 15)**.

- *mass conservation (C in different components, salinity, alkalinity, other ocean tracers)*

The model is mass conserving in the ocean for alkalinity and phosphate **(p23, line3-5)**. There is a net loss of carbon from the ocean, accounted for by the carbon flux into the atmosphere, but the magnitude is similar in magnitude to other CMIP5 models. (**p23, line 10-12**)

- *equilibration of pools in an emission-driven simulation*

We have performed tests of emission-driven simulations by including a flux correction to account for the non-zero fluxes diagnosed from the concentration-driven simulation and can achieve relatively stable integrations. We have not performed an emissions-driven case without flux correction because we know this would give unrealistic drifts in atmospheric CO_2 and consequent trends in carbon fluxes.

- *gross CO2 exchange fluxes, predicted vs. observed/estimated*
For land, different aspects of the gross CO2 exchange fluxes are presented in both parts of the study, with comparison against observations and other CMIP5 models predominantly in Part 2 since this evaluates the model behaviour under present-day conditions for which observations (or observation-based products) are available. Different aspects of the sea-air CO_2 fluxes are assessed in both this and the companion paper.

- *temperature fields (land surface and SST)*
A summary statistic for SST is already available in Fig 12.
Figure 2 will be replaced by the spatial distribution of land surface temperature difference between the progLAI and presLAI simulations **(new Fig 2)** with the original Figure 2 **(now Fig 16)** being moved to an appendix.

- *surface albedo*
We do not think there is a clear need to show surface albedo in this paper, given other priorities.

- *sea ice cover*
- *meridional overturning*
For assessing the model we have added figures for sea-ice area cover **(Fig 4)**, mixed layer depth (**Fig 3**), and zonal averaged ocean sections of DIC, ALK, phosphate and oxygen (**Fig 15**).

- *vegetation and soil C distribution and total pool sizes*
These are compared with observations in Part 2 (Ziehn et al.).

- *CO2 seasonality at different locations where observations are available (This is kind of an ultimate test, and is technically possible given that the UM model, in emission-driven setup, transports CO2 through the atmosphere and that the land model simulates NEE across space.)*
We have modified the atmospheric model so that even in a concentration-driven case we simulate the contribution of the land and ocean carbon fluxes to atmospheric CO_2 as separate passive tracers. We present the resulting atmospheric CO_2 seasonality in Part 2 (Ziehn et al.) and show that it compares reasonably well to observations.

- *other "standard" benchmarks (Benchmarking of coupled models has been a high priority for years now and helpful tools are freely available. See e.g., ESMValTool by Eyring et al., 2015, GMD).*
We are certainly interested in making use of ESMValTool and/or iLamb in future but currently do not have sufficient time to explore those options.

- *Open access: Not satisfied, in that the model code used to produce the results presented here is not available. Code for individual components may be accessed, but not for all components. Some links provided are inactive.*
The inactive link is for the MOM code. This will be corrected. **(p35, line7)**

- *Provide a very general description of some model characteristics, deficiencies and limitations (e.g. prescribed phenology, fixed N fixation and P weathering), to give at least a feeling for what the model can and cannot do. The balance between generality and detail in section 2 is not appropriate. E.g., Eq. 1 and 2 are unnecessary. It is ok to refer to other publications where these components are described.*

We will revise section 2, taking these comments into account. Most of the physical model detail (Section 2.1), which is not directly relevant to the carbon simulation, will be moved to the appendix

(**p31**). Equations 1 and 2 will be removed (**p7**). We will revise the conclusions to try to provide a clearer summary of the model characteristics, deficiencies and limitations. (**p28-31**)

- It's ok not to evaluate individual components in depth, but then the coupled system must be working ok (see above).
Given some of the issues identified in e.g. ocean NPP, we now present some ocean only simulations as a means of assessing how aspects of the simulation are degraded in the coupled system.(**Fig 14, p27**)

I hope my critical review helps to improve this manuscript. In many instances, the material and results are already available and a presentation with a focus on the most important aspects of what a coupled ESM should be able to simulate would much improve the present manuscript. This would lead to a convincing and transparent presentation of key features and variables, e.g. some of the ones I have listed above.
Thanks for the review and we have tried to fully address your comments.

SPECIFIC POINTS
- In abstract, it needs to be made clear what type of simulations are used for evaluation (forcing? emission/concentration-driven?) and against what it is evaluated.
This information will be added to the abstract. (**p2, line 11**; **p2, line 14-19 rewritten to indicate where evaluation is between model versions or other models or includes observations or other models**)

- In abstract, refer to model components presented in Fig 1.
It is not clear to us whether the reviewer would like the model components explicitly mentioned in the abstract (i.e. UM7.3/CABLE/MOM4p1/WOMBAT etc) or whether the reviewer wishes Fig 1 to be referenced from the abstract. Given that it would be unusual to refer to a figure from the abstract, we will add the component model names (**p2, line 5-8**).

- Introduction puts strong emphasis on climate-carbon cycle feedbacks. However, the paper does not address feedbacks (constant atmospheric CO2).
Agree, and we will re-write the introduction to highlight the usefulness of both concentration-driven and emissions-driven simulations (**p3, line 13-22**). We will also be clearer about why the concentration driven case is presented here. **(p4, line 23-25)**

- Many different setups may be chosen for comparison of effects. It remains unclear why prescribed and interactive LAI are given such an emphasis.
As noted above, this case was chosen because one configuration does not change the climate and the other does. This would be clearer if we had described our reasoning earlier in the paper. It will now be included towards the end of the introduction. (**p4, line 25-28)**

- Description of model configuration not sufficient: concentration of GHGs, albedo, areosol, solar radiation, other radiative forcing to drive simulation?
This information will be added to the model configuration section and if required a new subsection describing input files for the atmosphere will be added. For the physical model, the configuration generally follows that used for the ACCESS1.3 CMIP5 submission (except background stratospheric volcanic forcing) and it may be appropriate to explicitly reference relevant documentation of those simulations. **References added and differences noted, p11, line 15-22**

- To initialise the model prescribed observational DIC and Alk are used or variable values are "taken from identical test simulations", and no spin-up is done —> how does this work? Identical test simulations with 100% identical setup?}

Ocean Oxygen, Phosphate, DIC and Alk fields were initialized based on observations and a control run was run for 1000 years before starting the historical simulation. The text “taken from repeated test simulations” was referring to land carbon pool initialisation rather than ocean carbon, and the impact of that initialisation is noted when comparing the equilibration of the PresLAI and ProgLAI cases **(p19, line 5-7).**

- *C conservation in land C cycle: Why not 100% satisfied? Could this be a bug in the code? Numerical precision not sufficient? Or is this linked with the fact that CABLE does not simulate land C loss from disturbance (see p. 8071, l.1)? (this confused me anyway...)*
It is an inconsistency in the code in circumstances where the leaf carbon pool gets smaller than a minimum LAI value prescribed for each pft. This allows leaf respiration to exceed GPP which is unrealistic. Further explanation will be provided in the manuscript. (**p18, line 19-20**)

Manuscript prepared for Geosci. Model Dev. Discuss.
with version 2014/09/16 7.15 Copernicus papers of the LaTeX class copernicus.cls.
Date: 20 April 2016

The carbon cycle in the Australian Community Climate and Earth System Simulator (ACCESS-ESM1) – Part 1: Model description and pre-industrial simulation

R. M. Law[1], T. Ziehn[1], R. J. Matear[2], A. Lenton[2], M. A. Chamberlain[2], L. E. Stevens[1], Y. P. Wang[1], J. Srbinovsky[1], D. Bi[1], H. Yan[1], and P. F. Vohralik[3]

[1]CSIRO Oceans and Atmosphere, PMB 1, Aspendale, Victoria, Australia
[2]CSIRO Oceans and Atmosphere, Hobart, Tasmania, Australia
[3]CSIRO Manufacturing, Lindfield, New South Wales, Australia

Correspondence to: R. M. Law (rachel.law@csiro.au)

Abstract

Earth System Models (ESMs) that incorporate carbon-climate feedbacks represent the present state of the art in climate modelling. Here, we describe the Australian Community Climate and Earth System Simulator (ACCESS)-ESM1~~that combines existing ocean and land carbon models into the physical climate model to simulate exchanges of carbon between the land, atmosphere and ocean~~, which comprises atmosphere (UM7.3), land (CABLE), ocean (MOM4p1), and sea-ice (CICE4.1) components with OASIS-MCT coupling, to which ocean and land carbon modules have been added. The land carbon model (as part of CABLE) can optionally include both nitrogen and phosphorous limitation on the land carbon uptake. The ocean carbon model (WOMBAT, added to MOM) simulates the evolution of ~~nitrate~~phosphate, oxygen, dissolved inorganic carbon, alkalinity and iron with one class of phytoplankton and zooplankton. ~~From two~~ We perform multi-centennial ~~simulations of the~~ pre-industrial ~~period with~~ simulations with a fixed atmospheric CO_2 concentration and different land carbon model configurations ~~, we~~ (prescribed or prognostic leaf area index). We evaluate the equilibration of the carbon cycle and present the spatial and temporal variability in key carbon exchanges. ~~For the land carbon cycle,~~ Simulating leaf area index results in a slight warming of the atmosphere relative to the prescribed leaf area index ~~is simulated reasonably, and seasonal carbon exchange is well represented. Interannual variations of~~ case. Seasonal and interannual variations in land carbon exchange are ~~relatively large,~~ sensitive to whether leaf area index is simulated, with interannual variations driven by variability in precipitation and temperature. We find that the response of the ocean carbon cycle shows reasonable agreement with observations ~~and very good agreement with~~ with similar realism to existing Coupled Model Intercomparison Project (CMIP5) models. While our model ~~over estimates surface nitrate~~ overestimates surface phosphate values, the global primary productivity agrees well with observations. Our analysis highlights some deficiencies inherent in the carbon models and where the carbon simulation is negatively impacted by known biases in the underlying physical model and consequent limits on the applicability of this model version. We conclude the study with

a brief discussion of key developments required to further improve the realism of our model simulation.

1 Introduction

Over recent decades many climate models have evolved into ~~earth system models~~ Earth System Models (ESMs), a term used to identify models that simulate biogeochemical cycles and their interaction with human and climate systems. Of principal concern is the carbon cycle. Anthropogenic emissions of carbon lead to increased concentrations of atmospheric carbon dioxide (CO_2). This directly impacts uptake of carbon by the land and ocean systems and warms the climate. Climate warming, in turn, perturbs the carbon uptake, typically leading to reduced carbon uptake and a positive feedback on warming. This climate-carbon feedback was first explored by Cox et al. (2000) and Friedlingstein et al. (2001) and compared across models in Friedlingstein et al. (2006). This model intercomparison confirmed that all models gave a positive carbon-climate feedback but the magnitude of that feedback was very variable across models.

While ESM simulations with the full carbon cycle and an interactive atmosphere ('emissions-driven simulations') are essential for quantifying the carbon-climate feedbacks, simulations with a fixed atmospheric CO_2 ('concentration-driven') are also valuable. These simulations are used to diagnose land and ocean carbon exchange with the atmosphere based on a prescribed atmospheric history of CO_2 and any associated climate impacts of those atmospheric CO_2 changes. Thus the temporal evolution of carbon exchange can be evaluated for a range of future atmospheric CO_2 trajectories. This simpler concentration-driven mode for ESM simulations removes any direct impact of the carbon cycle on the climate simulation with indirect impacts only occuring through possible changes to the land surface characteristics such as leaf area index.

The Coupled Model Intercomparison Project (CMIP5) (Taylor et al., 2012) included additional model output ~~and extra model~~ from concentration-driven simulations and extra emissions-driven simulations for those models that could simulate the carbon cycle. Evalu-

ations were conducted of the concentration-driven model simulated carbon fluxes over the historical period (Anav et al., 2013) and the relationship of land carbon fluxes to different climate variables (Shao et al., 2013). Future carbon fluxes were compared across models for simulations with prescribed atmospheric CO_2 (Jones et al., 2013) and emissions-driven simulations (Friedlingstein et al., 2014). The range of results for the emissions-driven simulations was similar to that found by Friedlingstein et al. (2006) with the main cause of the large range being differences in the land carbon cycle projections. Feedback analysis was conducted by Boer and Arora (2012) and Arora et al. (2013).

The Australian Community Climate and Earth System Simulator, ACCESS, has been developed over recent years to meet both the numerical weather prediction (Puri et al., 2013) and climate simulation needs (Bi et al., 2013b) of the Australian Bureau of Meteorology, CSIRO and Australian university researchers. For climate needs, the initial aim was to put together a physical coupled climate model for participation in CMIP5. A second aim is to add the carbon cycle and implement an atmospheric chemistry scheme. Two versions of ACCESS participated in CMIP5 (Dix et al., 2013), ACCESS1.0 and ACCESS1.3 (Bi et al., 2013b), differing in their atmosphere model settings and land surface scheme. Development of the earth system version of ACCESS, denoted ACCESS-ESM1, is based on the ACCESS1.4 physical climate model, an updated version of ACCESS1.3 (Fig. 1).

This paper documents the components of ACCESS-ESM1 (Fig. 1), relative to previously published versions. Thus we note the relatively minor physical model differences between ACCESS1.3 and ACCESS1.4 (Appendix A) as well as the addition of the carbon components to ACCESS ~~,~~ (Sects. 2.2, 2.3, 2.4), to give the ~~ESM configuration, ACCESS-ESM1 as well as noting the physical model differences between ACCESS1.3 and ACCESS1.4. Model~~ current ESM configuration. The model configuration and model inputs required to run CMIP5-type carbon simulations are presented ~~, along with analysis of the behaviour of the~~ in Sect. 3. Evaluation of the ACCESS-ESM1 model is divided between this paper and part 2 of this study (Ziehn et al., 2016).

Here we focus on simulations under pre-industrial conditions and prescribed atmospheric CO_2~~. In particular, we focus our presentation on showing and assessing the~~

carbon flows in the land and , which should allow the simulated carbon cycle to equilibrate and provides the simplest case for a first evaluation of the model performance. Two land carbon configurations are compared, using prescribed or prognostic leaf area index (LAI). These were chosen because simulating LAI will have an impact on the carbon exchanges between the land, atmosphere and ocean . A companion paper, Ziehn et al. (2016)evaluates simulations covering the historical period climate simulation even with prescribed atmospheric CO_2 (Sect. 4.1). We then characterise the simulated carbon cycle behaviour, with the focus for land carbon on equilibration and variability (Sect. 4.2). Understanding the sensitivity of land carbon fluxes to natural climate variability may be useful for interpreting the response of land carbon fluxes to externally forced climate change, as well as for model evaluation. For ocean carbon, we focus our evaluation (Sect. 4.3) on equilibration and comparison against observations and other models where this is valid under pre-industrial conditions. In Ziehn et al. (2016), evaluation is for a concentration-driven historical simulation (1850–2005), while allowing a more extensive comparison against present-day observations, particularly for the land carbon cycle. ACCESS-ESM1 simulations for future periods (2005–2100) and emissions-driven simulations will be presented elsewhere.

2 ACCESS-ESM1 model description

ACCESS-ESM1 comprises the ACCESS1.4 physical climate model (Sect. 2.1), with new capability to simulate the carbon cycle. Land carbon fluxes (Sect. 2.2) are simulated as part of the Community Atmosphere Biosphere Land Exchange (CABLE) model which includes a module to simulate carbon exchange between land carbon pools, with the optional inclusion of nutrient limitation. Ocean carbon fluxes (Sect. 2.3) are simulated by the World Ocean Model of Biogeochemistry And Trophic-dynamics (WOMBAT). Versions of CABLE and WOMBAT have been documented previously (e.g., Kowalczyk et al., 2006; Oke et al., 2013). Hence the descriptions below are mostly limited to any model developments since the earlier work and specifics of the model implementation in the ACCESS-ESM1 context.

The focus is on the carbon fluxes from the land and ocean that are input to the atmosphere (Sect. 2.4), either actively influencing climate through the atmospheric CO_2 field or as passive tracers for comparison with observed atmospheric CO_2.

2.1 Physical model: ACCESS1.4~~compared to ACCESS1.3~~

~~As described in Bi et al. (2013b) and illustrated in~~ The physical model to which we are adding the carbon cycle is designated ACCESS1.4. As shown in Fig. 1, the atmospheric component of ACCESS1~~.3~~ .4 is the UK Met Office Unified Model (UM) (Martin et al., 2010; The HadGEM2 Development Team, 2011) to which the land surface model, CABLE, is directly coupled; the ocean component is a version of the NOAA/GFDL Modular Ocean Model (MOM4p1) (Griffies, 2009) and sea-ice is modelled using the LANL CICE4.1 model (Hunke and Lipscomb, 2010) with coupling of the ocean and sea-ice to the atmosphere with the OASIS coupler (Valcke, 2013). The ACCESS configuration of the ocean and sea-ice components, ACCESS-OM, is described in Bi et al. (2013a) with CMIP5 evaluations documented in Marsland et al. (2013) and Uotila et al. (2013). The ocean-only configuration of ACCESS has been extensively used to explore intrinsic variability in the ocean and the role it may play in decadal variability (e.g. O'Kane et al., 2013).

~~The physical model to which we are adding the carbon cycle is derived~~ ACCESS1.4 is a minor upgrade from ACCESS1.3~~and designated ACCESS1.4~~, which was used for CMIP5 and extensively documented (e.g. Bi et al., 2013b; Dix et al., 2013; Kowalczyk et al., 2013). ACCESS1.4 addresses a number of issues that were identified during the analysis of the ACCESS1.3 CMIP5 simulations and also includes an updated version of CABLE (CABLE2). ~~Changes made to CABLE are discussed in Sect. 2.2. Details of other changes between ACCESS1.3 and ACCESS1.4 are documented here.~~

2.1.1 ~~Atmosphere component~~

ACCESS1.3 used atmospheric physics settings similar to the Met Office Global Atmosphere (GA) 1.0 configuration (Hewitt et al., 2011) including the "PC2" cloud scheme (Wilson et al., 2008). A similar configuration is used for ACCESS1.4.

Analysis of ACCESS1.3 simulations showed almost no dust in the atmosphere (Dix et al., 2013); this was a consequence of changing the land surface scheme from the original UM land scheme to CABLE and freezing the ACCESS1.3 code version for CMIP5 before finalising dust settings. As described in Dix et al. (2013), the dust-uplift scheme used in the ACCESS models is based on Woodward (2001) and Woodward (2011), with dust being modelled for nine size bins with different particle diameters. Dust uplift can occur over bare soil and depends on wind speed, soil composition and volumetric soil-moisture content in the surface layer. Dust-uplift settings used by ACCESS1.4 for the tuneable parameters described in Woodward (2011) are friction-velocity tuneable constant $k_1 = 1.6$, soil-moisture tuneable constant $k_2 = 0.5$, overall scaling factor $C = 6.525$, maximum clay fraction for dust emissions of 0.1 and no preferential source term. These settings result in a global annual mean dust burden of 14.9 ± 1.3 (calculated over 160 from an ACCESS1.4 pre-industrial control simulation), which is broadly comparable to the AEROCOM multi-model median value of 15.8 for year 2000 conditions (Huneeus et al., 2011).

In addition to the change in dust, the ACCESS1.3 control simulation did not include background stratospheric volcanic forcing but this has been included in ACCESS1.4 simulations. Preliminary tests with the dust and vocanic forcing changes reduced the globally averaged surface air temperature relative to ACCESS1.3. Since an aim of ACCESS1.4 was not to change global-scale climate characteristics relative to ACCESS1.3, one of the parameters in the cloud scheme (FW_STD associated with the standard deviation of cloud water content) was increased from 0.700 in ACCESS1.3 Details of changes to 0.725 in ACCESS1.4. This resulted in a globally averaged surface air temperature in ACCESS1.4 that was similar to that obtained for ACCESS1.3. ACCESS1.4 also corrects a bug which zeroed the downward short-wave radiation over coastal sea-ice points for non-radiation timesteps. This reduced excess ice accumulation in ACCESS1.3 in some coastal regions such as the Canadian Archipelagos.

2.1.1 ~~Ocean component~~

~~While there are no changes in the ocean model version~~ the physical model between ACCESS1.3 and ACCESS1.4 ~~, there have been two changes in the configuration or parameter values. Firstly for ACCESS1.4, the background vertical diffusivity outside 20 S to 20 N has been increased from 0.5×10^{-5} to 1.0×10^{-5}, which is also consistent with the value used in ACCESS-OM. Secondly, the ocean absorption of penetrative solar radiation is now calculated using the diffuse attenuation coefficient of the downwelling photosynthetically available radiation (K_{dPAR}) rather than the downwelling spectral irradiance at wavelength 490 (K_{d490}). Since K_{dPAR} data covers a broader, more representative, spectrum of light, it is considered to be more appropriate for use in the ocean model and was also the dataset used in the standard ACCESS-OM configuration. Bi et al. (2013a) compares ACCESS-OM simulations using K_{dPAR} and K_{d490} and concludes that differences are mostly confined to the subsurface water between 40 S to 40 N with little impact on the deep ocean climate or the global ocean circulation and associated water volume transports.~~ are given in Appendix A.

2.1.1 ~~OASIS coupler~~

~~ACCESS1.3 used the OASIS3.2-5 coupler (Valcke, 2006). In ACCESS1.4, this is replaced by OASIS3-MCT (Valcke et al., 2013) which is designed to provide more efficient coupling for models running on many processors. For ACCESS1.4, this enables the simulation of about 7.2 model years per day (using 144 processors) compared to 5.4 model years per day for ACCESS1.3.~~

2.2 Land carbon model: CABLE

CABLE is a land surface model that simulates the fluxes of momentum, heat, water and carbon across the land-atmosphere interface. CABLE operates both in standalone mode (forced with prescribed meteorology) and coupled to atmospheric models (at least five different models to date, both global and regional). The history and sci-

entific core of CABLE version 1 is most fully described in Kowalczyk et al. (2006) with a summary description provided in the Appendix of Wang et al. (2011). ~~CABLE was initially implemented in~~ ACCESS1.4 and ACCESS-ESM1 use CABLE2.2.3 ~~at version 1.8 (CABLE1.8, Kowalczyk et al., 2013~~(Fig. 1). CABLE version 2 was designed to provide a consolidation of the standalone and ACCESS versions of CABLE into a single code repository with common science routines. In particular, this enabled the ACCESS version to optionally run with a biogeochemical module (Wang et al., 2010), which was initially developed for the standalone version.

~~ACCESS1.4 and ACCESS-ESM1 use CABLE2.2.3 (Fig. 1), but in ACCESS1.4 the biogeochemical module is not switched on. Apart from the inclusion of the biogeochemical module, CABLE2.2.3 has a number of small science changes and bug fixes from CABLE1.8 (used in ACCESS1.3). These dealt with occasional non-physical exchange coefficients, addressed some poor behaviour under very dry conditions, improved the water balance in the coupled system and ensured all CABLE variables were correctly being passed back into the ACCESS atmosphere e.g. for use by dry deposition. Often these changes could be shown to improve CABLE's performance in standalone mode for individual locations (e.g. at desert sites for the dry condition changes) but did not have broad-scale impacts when tested globally in atmosphere-only ACCESS simulations. Thus the assessment of the land surface impacts on the ACCESS climate for ACCESS1.3 (Kowalczyk et al., 2013) would also be applicable to ACCESS1.4 and ACCESS-ESM1 simulations. The improvements to the water balance approximately halved the drift in global ocean salinity in ACCESS1.4 compared to ACCESS1.3.~~

In ACCESS, CABLE is run for one or more tiles in each grid-cell with a non-zero land fraction. Each tile represents a different vegetated or non-vegetated surface type with a number of CABLE input parameters being surface type dependent (Sect. 3.1.1). Each tile is modelled with a separate soil column beneath the surface. The biogeochemistry module, denoted CASA-CNP, simulates the flow of carbon, and optionally, nitrogen and phosphorus between three plant biomass pools (leaf, wood, ~~roots~~root), three litter pools (metabolic, structural, coarse woody debris) and three organic soil pools (microbial, slow, passive), one

inorganic soil mineral nitrogen pool and three other phosphorus soil pools (labile, sorbed, strongly sorbed).

The flux of carbon from the land to the atmosphere has two components, net ecosystem exchange (NEE) and fluxes due to disturbance (e.g. fire) and land-use change. Currently CABLE simulates the former ~~, as the difference between respiration and photosynthesis,~~ but not the latter. ~~Thus~~

$$\mathrm{NEE} = -1 \times \mathrm{NEP}$$

~~and net ecosystem production (NEP) is the difference between gross~~

Gross primary production (GPP) and ~~plant (or autotrophic, R_a) and soil (or heterotrophic, R_h) respiration~~

$$\mathrm{NEP} = \mathrm{GPP} - R_\mathrm{a} - R_\mathrm{h} = \mathrm{NPP} - R_\mathrm{h}$$

~~where NPP is net primary production.~~

~~GPP and~~ leaf maintenance respiration are calculated every time step using a two-leaf (sunlit and shaded) canopy scheme (Wang and Leuning, 1998).

$$\mathrm{GPP} = f(\mathrm{LAI}, v_\mathrm{cmax}, j_\mathrm{max}) \tag{1}$$

where LAI is leaf area index, v_cmax is the maximum rate of carboxylation and j_max is the maximum rate of potential electron transport. LAI may be prescribed or simulated, with simulated (prognostic) LAI being dependent on the size of the leaf carbon pool (c_leaf) and the specific leaf area (SLA), which is a vegetation dependent parameter:

$$\mathrm{LAI} = \max(\mathrm{LAI}_\mathrm{min}, c_\mathrm{leaf} \times \mathrm{SLA}) \tag{2}$$

where the max function ensures a vegetation dependent minimum LAI ($\mathrm{LAI}_\mathrm{min}$). Section 4.2.1 notes an unintended impact of this minimum LAI constraint. v_cmax and j_max are vegetation dependent parameters for carbon only simulations, but when nutrient limitation

is active, v_{cmax} and j_{max} become dependent on leaf nitrogen (n_{leaf}) and phosphorus to nitrogen ratio (p_{n}) (Zhang et al., 2013; Wang et al., 2012):

$$v_{\text{cmax}} = (a + bf(p_{\text{n}})n_{\text{leaf}}) \times c \tag{3}$$

$$j_{\text{max}} = 2v_{\text{cmax}} \tag{4}$$

where a and b are vegetation type dependent empirical coefficients taken from Kattge et al. (2009) and c is effectively used as a tuning parameter (Supplement, Table S1). For evergreen broadleaf forest $f(p_{\text{n}})$ is expressed as:

$$f(p_{\text{n}}) = 0.4 + 9p_{\text{n}} \tag{5}$$

and set to one for other vegetation types due to the lack of data (Zhang et al., 2013).

Daily mean GPP and leaf respiration are passed into the biogeochemical module which is run once per day to calculate the remaining respiration fluxes and the carbon flow between pools. The fractions of GPP allocated to each vegetation pool are vegetation dependent parameters which, for non-evergreen vegetation types, are also dependent on leaf phenology phase (Wang et al., 2010). The phenology phase is prescribed by latitude and vegetation type and is based on remote sensing data (Zhang et al., 2004, 2005).

Maintenance respiration of woody tissue and roots and growth respiration are calculated as a function of mean daily air temperature and tissue nitrogen amount. Default carbon to nitrogen and nitrogen to phosphorus ratios are used when nitrogen and/or phosphorus are not simulated. Growth respiration is calculated daily as a proportion of the difference between daily GPP and plant maintenance respiration, with the proportion being a function of leaf nitrogen to phosphorus ratio (Zhang et al., 2013). Microbial respiration from decomposition of litter and soil carbon is also calculated daily and depends on the amount of organic carbon (or substrate quantity), the nitrogen to carbon ratio of organic carbon in litter or soil (substrate quality), and soil temperature and moisture (Kelly et al., 2000). We used a Q10-type function to describe the dependence of microbial respiration on soil temperature, although other functions can also be used (Exbrayat et al., 2013).

Since plant and soil respiration rates are only calculated daily, CABLE in ACCESS-ESM1 is not expected to realistically simulate the diurnal cycle of the net land carbon flux to the atmosphere, and we restrict our analysis to monthly or longer timescales.

Carbon should be conserved across the land carbon system, that is the net flux to the atmosphere over a given time period should equal the change in the total carbon across all carbon pools over that same period. A carbon conservation check is presented in Sect. 4.2.1.

CABLE with CASA-CNP has been used in a number of offline applications, where meteorological forcing is prescribed, (e.g., Huang et al., 2015) as well as in a low resolution earth system model in atmosphere-only simulations (Zhang et al., 2011, 2013; Wang et al., 2015) or in atmosphere-ocean coupled simulations (Zhang et al., 2014). Experience from these studies has guided configuration and parameter choices for CABLE in ACCESS-ESM1 (Sect. 3).

2.3 Ocean carbon model: WOMBAT

The Whole Ocean Model of Biogeochemistry And Trophic-dynamics (WOMBAT) model is based on a NPZD (Nutrient, Phytoplankton, Zooplankton and Detritus) model with the additions of bio-available iron limitation (Fe), dissolved inorganic carbon (DIC), calcium carbonate ($CaCO_3$), alkalinity (ALK), and oxygen (O). At present WOMBAT includes only one class each of phytoplankton and zooplankton. All biogeochemical (BGC) tracers are calculated on the same grid as temperature. The equations of WOMBAT are given in Oke et al. (2013, Appendix B) and the parameters used in this simulation are given in Table 1. In our simulations our nutrient is phosphate and hence we do not explicitly simulate ~~nitrate. In our later comparisons we convert phosphate to nitrate using the stoichiometric ratios of Anderson and Sarmiento (1994)~~the nitrogen cycle.

In this model we include two DIC tracers: natural and anthropogenic DIC. These two DIC tracers only differ in the atmospheric CO_2 concentration used in the air–sea flux calculation. For the natural DIC, the atmospheric CO_2 was kept at 285 ppm while for anthropogenic DIC the atmospheric CO_2 increases according to the historical or future atmosphere con-

centration. At the surface we calculate the air–sea exchange of the two carbon tracers and oxygen following Lenton and Matear (2007), which uses the difference in partial pressure between the ocean and atmosphere, the simulated sea-ice concentrations, and the wind-speed squared and temperature dependent gas exchange coefficient following Wanninkhof (1992). We used the OCMIP3 protocol to compute ocean pCO_2 from the simulated temperature, salinity, phosphate, DIC and ALK fields. WOMBAT simulates the biological production and export of particulate organic carbon (detritus) and calcium carbonate from the photic zone and its subsequent remineralization in the ocean interior. The remineralization of particulate organic matter occurs through prescribed remineralization and sinking rates. The model maintains particulate organic matter and calcium carbon sediment pools so that any particulate material reaching the sediments is remineralized back into the overlying water at the same remineralization rate as the water column values. The sediment pools are included to improve numerical stability of the ocean carbon module by preventing the instantaneous remineralization of particulate material in the deepest layer of the model.

2.4 Atmospheric carbon dioxide

ACCESS-ESM1, mostly through capability inherited from the Met Office Unified Model, has the option of running with or without interactive CO_2. When interactive CO_2 is selected, a three-dimensional atmospheric CO_2 field is simulated and ~~atmospheric~~ CO_2 is transported through the atmosphere. This CO_2 field influences the radiation calculation in the model as well as the calculation of the land and ocean carbon fluxes through CABLE and WOMBAT respectively. The atmospheric CO_2 field is, in turn, dependent on the land and ocean carbon fluxes into or out of the atmosphere, along with any additional prescribed (e.g. anthropogenic) carbon flux. In this mode, ACCESS-ESM1 can simulate any climate-carbon feedback that might result from ~~increasing~~ changing anthropogenic carbon fluxes. This mode is used for the CMIP5 ~~"~~emissions-driven ~~"~~ simulations. While maintaining an interactive 3-D CO_2 field, an additional switch in ACCESS-ESM1, allows the model radiation scheme to revert to ~~responding to~~ a prescribed (usually spatially constant) atmospheric CO_2

mixing ratio. This enables simulations to be run that separate the direct effects of increasing atmospheric CO_2 on simulated carbon fluxes from how the climate affects carbon fluxes.

When ACCESS-ESM1 is run without interactive CO_2, the radiation scheme and carbon flux models are forced with a common prescribed atmospheric CO_2 concentration. This might be constant in time for a pre-industrial control run, or increasing in time for historical or future scenarios. Many of the CMIP5 simulations run in this mode. When running in this way, we have also enabled the model to pass the land and ocean carbon fluxes into two of the passive tracer fields that are part of the Unified Model code. These tracers are transported through the atmosphere and allow us to assess the separate contributions of land and ocean carbon fluxes to features in observed atmospheric CO_2 such as the seasonal cycle or interannual variability.

The atmospheric transport of CO_2 does not perfectly conserve carbon. To ensure that carbon is conserved in the atmosphere, a mass fixer has been applied as described in Sect. 2.2.2 of Jones et al. (2011).

3 Model configuration

The ACCESS-ESM1 atmosphere is run with a horizontal resolution of 1.875° longitude × 1.25° latitude, and with 38 vertical levels. The land surface has the same horizontal resolution but each grid-cell comprises multiple tiles of different vegetation type. The ocean horizontal resolution is nominally 1°, with latitudinal refinements around the equator (0.33 between 10° S and 10° N) and the Southern Ocean (ranging from 0.25 at 78° S to 1° at 30° S), and a tripolar Arctic north of 65° N (Bi et al., 2013a). There are 50 ocean vertical levels with a nominal 10 m thickness in the upper ocean. In general the physical model configuration and forcings follow that used for the ACCESS1.3 CMIP5 simulations (Bi et al., 2013b; Dix et al., 2013), except that the ACCESS1.3 pre-industrial simulation did not include background statospheric volcanic forcing. For ACCESS-ESM1, this forcing has been applied uniformly in time and space as an aerosol optical depth of 0.013, the mean value of the stratospheric volcanic forcing applied from 1850-2000

in the ACCESS-ESM1 historical simulation. Atmospheric CO_2 is prescribed at 285 ppm throughout the pre-industrial simulation.

As noted above, CABLE can simulate land carbon fluxes with or without nutrient limitation. Here we have chosen to run CABLE in the "CNP" configuration, based on results from some low resolution ESM studies. Zhang et al. (2014) assessed the sensitivity of allowable emissions to nutrient limitation comparing cases running the carbon cycle alone (C), carbon and nitrogen (CN) or carbon, nitrogen and phosphorus (CNP). Depending on the scenario and time period considered, the CN case reduced land carbon uptake by 35–40 % relative to the C case, with a further 20–30 % reduction in the CNP case. The CN and CNP cases were within the uncertainty range of ~~observed~~ estimated global land carbon uptake for the historical period, as compiled by Zhang et al. (2014). Zhang et al. (2013) assessed the interaction of land cover change with nutrient limitation. Again the CNP case gave land carbon uptake more consistent with observations than the C only case.

For most of the work described here, two sets of simulations have been performed. In the first set, ~~leaf area index~~ LAI is prescribed and there should be no interaction between the carbon cycle and the climate simulation (given that atmospheric CO_2 is prescribed in these simulations). In the second set, LAI is prognostic and dependent on the size of the leaf carbon pool. In this case, the change in LAI has an impact on climate through its influence on radiation absorption and momentum, heat and moisture fluxes. The climate impact will be briefly examined in Sect. 4.1. The ocean carbon model configuration was the same for both the prescribed LAI and prognostic LAI simulations.

3.1 Input files

3.1.1 Land

Most of the input files and parameter settings (Supplement) for the biophysical component of CABLE were as described in Kowalczyk et al. (2013) including the LAI used in our prescribed LAI simulation. Note that the same LAI is used for all vegetation types within a grid-cell.

Differences between the model configuration here and Kowalczyk et al. (2013) are (a) a slight difference in the vegetation distribution used and (b) a change in the leaf optical property parameters. Thirteen surface types are differentiated: four forest types (evergreen needleleaf, evergreen broadleaf, deciduous needleleaf, deciduous broadleaf), six shrub and grass types (shrub, C3 grass, C4 grass, tundra, crop, wetland) and three non-vegetated types (lakes, ice, bare ground). As in Kowalczyk et al. (2013) the vegetation distribution is derived from Lawrence et al. (2012) but where Kowalczyk et al. (2013) restricted each grid-cell to three dominant vegetation types, here vegetation types are selected based on whether they ever occur at greater than 10 % of the grid-cell at any time between 1850 and 2100 (under any CMIP5 historical or RCP scenario). This results in a variable number of vegetation types per grid-cell, from one to seven. While the simulations presented here do not account for land-use change and are all run with a pre-industrial (1850) vegetation distribution, the vegetation dataset has been constructed to allow further simulations in which the impacts of land-use change are modelled. The vegetation distribution includes a small number of wetland tiles but due to an incorrect setting for CASA-CNP, these were effectively excluded from the simulation of carbon fluxes. The small area involved means there is no significant impact on any simulation results presented here. The change in leaf optical properties (reflectance and transmission) for ACCESS-ESM1 was designed to be more consistent with the snow-free soil albedo used in ACCESS. The change was made to improve the low albedo simulated by ACCESS1.3 (Kowalczyk et al., 2013).

Additional input files are required for the biogeochemistry module of CABLE and these are based on Wang et al. (2010). Parameters (Supplement) such as the fraction of ~~NPP~~ net primary production allocated to different pools and turnover times are specific to each vegetation type and are set from literature values or tuned based on offline simulations (Wang et al., 2010). We use the same prescribed leaf phenology as Wang et al. (2010) which gives the timing of green-up and leaf fall by latitude for all vegetation types except evergreen trees. We note here the limitation of using present day leaf phenology for pre-industrial simulations and the inability of the model to simulate a changing growing season with changing climate.

To simulate nitrogen and phosphorus requires nitrogen deposition and fixation, phosphorus from weathering and from dust and soil order, to distinguish soils of different mineralogy and age. These are all taken from Wang et al. (2010), re-gridded for the ACCESS-ESM1 model resolution and are representative of present-day conditions with no temporal variation. Nitrogen and phosphorus fertiliser ~~application rates are also taken from Wang et al. (2010) and~~ is applied to all crop tiles ~~(~~at a present-day application rate taken from Wang et al. (2010). Given a smaller crop area in the 1850 vegetation distribution used ~~here)~~in all simulations than for present-day, this gives a total fertiliser application that is a compromise between pre-industrial, present-day and future fertiliser use.

3.1.2 Ocean

The initial conditions for phosphate (P) and oxygen (O_2) are derived from the 2005 version of the World Ocean Atlas (WOA2005; Garcia et al., 2006a, b). Phytoplankton in the top 100 m was initialised using Chlorophyll (Chl a) taken from a climatology of SeaWIFS (1997–2008) and then scaled to Phosphorus units using the ratio P : Chl $a = 1/16\,\mathrm{mmol\,m^{-3}}$ P : $1.59\,\mathrm{mg\,m^{-3}}$ Chl a. Zooplankton was initialised as 0.05 of the initial phytoplankton concentrations. The initial field for Iron (Fe) was taken from a 500 year integration of a coarser resolution simulation of WOMBAT. Pre-industrial DIC and ALK are initialised from the Global Ocean Data Analysis Project (GLODAP, Key et al., 2004).

3.2 Spin-up

There was no formal spin-up of the carbon cycle before the ACCESS-ESM1 pre-industrial control run was started. The land carbon pools were initialised at values taken from repeated test simulations using the prognostic LAI configuration. The ocean BGC initial fields come from the observed climatology as described in the previous section. Offline land simulations and ocean-only simulations were explored to aid in the spin-up process but neither produced a satisfactory result at the time the pre-industrial run was started. This partly re-

flected the significant and evolving change of the mean climatology of the land, ocean and atmosphere from the present-day state.

4 Results: pre-industrial control run

In this section results from two ACCESS-ESM1 pre-industrial control simulations will be characterised and compared. Each simulation presented here used prescribed (rather than interactive) atmospheric CO_2 set to 285 ppm. The first simulation ran CABLE with prescribed leaf area index, which we denote "PresLAI" and the second simulation ran CABLE with prognostic LAI, denoted "ProgLAI". The ocean carbon configuration was the same for both simulations, using the ocean parameter set in Table 1. Both these simulations have been run for 1000 years.

A brief analysis of the simulated climate is presented first (Sect. 4.1), focussing on how the climate simulation is impacted in the ProgLAI case and on climate variables most relevant to the carbon cycle simulation. For land carbon (Sect. 4.2), the analysis of the pre-industrial control run focusses on carbon conservation, equilibration, and variability, both spatially and temporally. We do not compare land carbon fluxes with observations ~~as~~ because there are no pre-industrial datasets and this is addressed in the assessment of the historical simulation presented in Ziehn et al. (2016). For ocean carbon (Sect. 4.3), the analysis of the pre-industrial control run focusses on the temporal evolution of global air–sea fluxes and primary productivity, and presents the mean state ~~, and an estimate of interannual variability~~of key ocean biogeochemical fields. The ocean carbon-cycle response is compared to observations where relevant, and with the results of CMIP5 models. Ziehn et al. (2016) presents spatial and seasonal distributions of ocean net primary production and the seasonality of air-sea carbon flux. The impact of ~~the~~ land and ocean carbon fluxes on atmospheric CO_2 is included in Ziehn et al. (2016) for comparison with observed atmospheric CO_2.

~~A brief analysis of the simulated climate is presented first (Sect. 4.1), noting primarily how the climate simulations are impacted by any carbon cycle configuration choices (e.g.~~

prognostic LAI) and any deficiencies in the climate simulation that may cause problems for the carbon simulation.

4.1 Climate

Relative to the range of CMIP5 models, the two ACCESS submissions, ACCESS1.0 and ACCESS1.3 produced similar results when various modelled atmospheric climate variables were compared against observations (e.g. Flato et al., 2013, Fig. 9.7). Here we compare the ACCESS1.4 and ACCESS-ESM1 In general, the pre-industrial climate simulations against that of for both configurations of ACCESS-ESM1 are very similar to that of ACCESS1.3 , using ACCESS1.0 to assess these relative differences. We calculate the root mean square difference (RMSD), similar to Gleckler et al. (2008), between each modelled field (F) and that modelled by ACCESS1.3 (R) for monthly mean values averaged across 100 of each pre-industrial simulation for all longitude (i) and latitude (j) and, depending on the variable, at different pressure levels:

$$\mathrm{RMSD}^2 = \frac{1}{W}\sum_i\sum_j\sum_t w_{ijt}(F_{ijt} - R_{ijt})^2$$

where t corresponds to the time dimension (12 months) and W is the sum of the weights (w_{ijt}) which, for the spatial domain, are proportional to the grid-cell area. We then normalise by the ACCESS1.0 RMSD:

$$\mathrm{RMSD}_{\mathrm{norm}} = \mathrm{RMSD}_{\mathrm{model}}/\mathrm{RMSD}_{\mathrm{ACCESS1.0}}$$

such that a value of 1 indicates that the simulated variable is as different from ACCESS1.3 as ACCESS1.0 is from ACCESS1.3 while values smaller than 1 indicate a simulation that is closer to that of ACCESS1.3. Figure 16 shows that for a range of atmospheric variables the normalised RMSD for ACCESS1.4 is generally around 0.3–0.4 indicating that the ACCESS1.4 climate simulation is much closer to ACCESS1.3 than ACCESS1.0 is to ACCESS1.3. This would be expected given the relatively small number of science changes between ACCESS1.3 (Bi et al., 2013b) and ACCESS1.4 . Likewise the (Appendix A).

Running ACCESS-ESM1 ~~simulation with prescribed LAI shows similar RMS differences from ACCESS1.3, implying little or no change from the ACCESS1.4 simulation when the carbon cycle is included but the atmospheric is prescribed. The RMS differences for ACCESS-ESM1 with prognostic LAI are generally similar or slightly larger than for the case with prescribed LAI, with the largest differences being for near surface and lower tropospheric temperature and geopotential height at 500 . This confirms that changing the LAI has a small impact on the climate simulation.~~

~~For surface air temperature, the prognostic LAI case~~ with prognostic LAI results in globally warmer ~~temperatures~~ surface air temperature ($14.59 \pm 0.11\,^{\circ}$C averaged over the final 300 years of the ProgLAI simulation compared to $14.22 \pm 0.10\,^{\circ}$C for the PresLAI case). The surface warming extends through the troposphere and is largest over northern high latitude continents (typically 1–2 °C) while over tropical forests the ProgLAI case is slightly cooler (around 0.5 °C) than the PresLAI case ~~.~~(Fig. 2a). The northern high latitude warming is more pronounced in winter than summer suggesting an interaction between LAI and snow. For example, larger LAI would mean less snow visible under the leaf canopy, a reduced albedo and a consequent higher temperature. The simulated prognostic LAI is presented in Sect. 4.2.3; lower prognostic than prescribed LAI generally appears to result in lower temperatures and vice versa~~. Note that the~~ , at least where the LAI changes are relatively small. A much reduced LAI appears to be associated with warming in some parts of the tropics. The different temperature impacts show that there is no simple relationship between LAI and temperature, rather LAI impacts on many components of the surface energy balance. We also note that the temperature differences triggered by changes in LAI are small compared to the tropical-polar temperature gradient and seasonal cycles of temperature ~~.~~(Fig. 2b) and both simulations give temperature distributions that are close to those derived from observations (Jones and Harris, 2014).

The ACCESS-ESM1 simulations of precipitation are similar to ACCESS1.3 and ACCESS1.4 (Appendix A). This means that precipitation biases identified in ACCESS1.3 (Kowalczyk et al., 2013) are also present in ACCESS-ESM1, in particular negative precipitation biases over India in June–August and over the Amazon in December–February

(their Fig. 9). These biases have implications for the sustainability of vegetation due to insufficient moisture (Sect. 4.2.1) with consequent impacts on the simulation of the land carbon cycle.

To provide a perspective on ~~how~~ the ocean dynamics ~~changes between ACCESS1.3 and ACCESS1.4 we compare~~ of ACCESS-ESM1, we show the global meridional overturning streamfunction~~and~~ , the annual maximum mixed layer ~~averaged over~~ depth and sea-ice area for the last 100 years of the ~~500 control simulations .~~ simulation. For these ocean diagnostics, the two ACCESS-ESM1 simulations are very similar and we only show the results from the simulation with prognostic LAI.

Global meridional overturning circulation ~~is very similar in the two simulations~~ from ACCESS-ESM1 (Fig. 3~~). One important difference is in the strength of the~~ a) shows a maximum strength in the Antarctic Bottom Water (AABW) cell ~~where ACCESS1.4 has a maximum strength~~ of 8 Sv, which is comparable to previous ACCESS simulations (Bi et al., 2013a). The maximum strength of the North Atlantic Deep Water cell is about 2~~2~~4 Sv~~less than ACCESS1.3. With reduced AABW formation and the associated Southern Ocean deep cell~~ , ~~ACCESS1.4 is slightly warmer in the deep ocean (up to 0.2 by the end of the control run) than ACCESS1.3,~~ which is ~~more consistent with observations (Boyer et al., 2009).~~ also comparable to other CMIP5 simulations.

The maximum mixed layer depth ~~is also very similar in the two simulations~~ of ACCESS-ESM1 shows maximum mixed layers deeper than 1000 m in the Ross and Weddell Seas and the North Atlantic (Fig. **??**3b). The ~~most significant difference occurs in the high latitude Southern Ocean where ACCESS1.4 has shallower depths in the Ross and Weddell Seas and deeper depths to the north of these seas. This difference accounts for the reduced AABW formation of ACCESS1.4. ACCESS-ESM1 maximum mixed layer depth (not shown) is very similar to ACCESS1.4, as expected since both model versions share the same ocean configuration. Both these diagnostics show the ocean dynamics of ACCESS1.4 (and consequently~~ Sub-Antarctic Zone is also a region where maximum mixed layer depths show regional maxima with mixed layer depths approaching 600 m, which is comparable to observations. Both the spatial pattern and magnitude of the maximum

annual mixed layer depths in the ACCESS-ESM1 ~~) is very similar to~~ simulation are comparable to previous ACCESS1.3 ~~and we can use the previous analysis of ACCESS1.3 (Marsland et al., 2013; Uotila et al., 2013) to help interpret our ocean simulation~~and 1.4 simulations (Marsland et al., 2013; Uotila et al., 2013).

~~Any climate model produces biases in its climate simulation when compared with observations. Some of these biases may also have implications for the simulation of the carbon cycle. Here we note two biases that impact on different components of the carbon cycle. Firstly, Kowalczyk et al. (2013) reported seasonal negative precipitation biases over India in June–August and over the Amazon in December–February for the ACCESS1.3 historical simulation. Similar biases are seen in all our ACCESS-ESM1 simulations , with implications for the sustainability of vegetation due to insufficient moisture (Sect. 4.2.1). Secondly salinity in the surface ocean has large regional biases (Bi et al., 2013b, Fig. 16), which produce surface alkalinity biases because alkalinity is strongly influenced by air–sea freshwater exchanges. These alkalinity biases will introduce biases in surface~~ To assess the ACCESS-ESM1 simulation of sea ice, we show the seasonal climatology of the northern and southern sea ice area from the last 100 years of the simulation (Figure 4a). In both hemispheres the seasonal climatology is similar to the observations but with a tendency to slightly under-estimate the sea ice area. Such behaviour is similar to other ACCESS simulations and other CMIP5 simulations (Marsland et al., 2013; Uotila et al., 2013). The simulated annual average sea ice area for ACCESS-ESM1 is similar to the observed values of $11.6 \pm 0.6 \times 10^{12} m^2$ and ~~air–sea flux of .~~ $11.6 \pm 0.5 \times 10^{12} m^2$ for the northern and southern hemispheres respectively Comiso (2000). The simulation shows much greater variability in the annual average in the southern hemisphere than the northern hemisphere (Fig. 4b).

4.2 Land carbon

4.2.1 Land carbon conservation

The conservation of land carbon has been checked across a sample 100 year period of the PresLAI and ProgLAI simulations (years 601–700, other 100 year periods give similar results). The change in total carbon across all carbon pools over the 100 years was compared with the net carbon flux to the atmosphere across the same period for each vegetated tile. The distribution of this carbon imbalance varied with vegetation type but was typically highly skewed~~with~~ ; negative values were in the range of -1.9 to 0 $g\,C\,m^{-2}$ over 100 years while a small number of positive imbalances ranged up to 1000–48000 $g\,C\,m^{-2}$ over 100 years. The large positive imbalances ~~, indicating~~ indicate that the change in carbon across the pools was smaller than the flux of carbon to the atmosphere.

~~If we choose~~ Based on the range of negative imbalances, we assume that $\pm 2\,g\,C\,m^{-2}$ over 100 years ~~as indicative of good carbon conservation , then~~ is indicative of the computational precision of the carbon conservation calculation. Using this criteria 85 % of vegetated tiles in the PresLAI simulation and 87 % of tiles in the ProgLAI simulation ~~meet this criteria~~show good carbon conservation. The shrub vegetation type has the smallest proportion of tiles meeting this criteria (45–62 %) followed by deciduous broadleaf in the PresLAI case (70 %) and C3 grass in the ProgLAI case (75 %).

Tiles with poor carbon conservation are characterised by zero or very low leaf carbon and possibly other highly depleted carbon pools. The magnitude of the carbon imbalance is well correlated (greater than 0.9) with a count of the number of months with zero leaf carbon across the 100 year period. The low leaf carbon often ~~appears to occur~~ occurs in regions with low rainfall. ~~It is likely that a poor simulation of rainfall~~ This can be illustrated by taking a transect along 76.9° E from 8.75-32.5° N across India (where rainfall is poorly simulated by the physical model~~in certain regions (e. g. India)~~). Rainfall is much larger at the northern and southern ends of the transect and badly underestimated in between. The leaf carbon pool for the crop vegetation type (which is present across the latitude range) follows the rainfall distribution with higher values at the ends of the transect than

in the middle (correlation with precipitation of 0.93). Clearly the low rainfall is leading to insufficient moisture to support plant growth. Effectively the plants die, but while this may be a realistic response to insufficient rainfall, it is now apparent that CABLE is not handling this situation in a self-consistent manner. In the PresLAI case, this is likely due to a lack of coupling between the LAI and the leaf carbon pool but this can also occur in the ProgLAI case because the model has been coded to enforce a minimum allowed LAI (dependent on vegetation type). Since the leaf respiration calculation is dependent on LAI, this leads to situations where leaf respiration becomes greater than GPP. Reformulating CABLE to better manage this situation is a high priority for future model development. The impact of the lack of carbon conservation on the overall model simulation will be noted where applicable in the analysis that follows (but is generally found to be small). and confined to relatively small regions. Given the land carbon calculation in each tile is independent, a lack of conservation in individual tiles does not adversely impact any other tiles.

4.2.2 Flux equilibration

The temporal evolution of the global land carbon fluxes over the 1000 years of simulation is shown in Fig. 5. In the ProgLAI case (Fig. 5a), GPP is slightly smaller than the summed respiration fluxes, with both showing a small drift to smaller values over the first 400–500 years. Variations between consecutive 25 year periods can be 1–2 $\mathrm{Pg\,C\,yr^{-1}}$ and are similar between GPP and summed respiration. The variability is smaller in the PresLAI case (Fig. 5b) when the feedback from the prognostic LAI is not included. In the PresLAI case the summed respiration fluxes decrease in time, particularly over the first 300 years. This is to be expected since the prognostic LAI configuration had been run for several hundred years in test runs before the start of the 1000 year simulation but this was not the case for the PresLAI run. Respiration takes longer to equilibrate than GPP because of its dependence on carbon pools with longer turnover times.

Figure 5c shows the 25 year mean NEE for the two model configurations. Again, after the initial adjustment of the PresLAI case, the ProgLAI case is more variable than the PresLAI one. Neither case equilibrates to zero; over the last 500 years of the simulation the global

NEE is 0.40 $\mathrm{Pg\,C\,yr^{-1}}$ for PresLAI and 0.14 $\mathrm{Pg\,C\,yr^{-1}}$ for ProgLAI. However tiles with poor carbon conservation contribute disproportionally to this global NEE with the largest NEE imbalances confined to relatively small regions in India and eastern tropical South America (Supplementary Figure 1). Excluding the 15 % of tiles with poor conservation, the NEE is reduced to 0.07 and 0.05 $\mathrm{Pg\,C\,yr^{-1}}$ for the PresLAI and ProgLAI cases respectively. In both cases, the evergreen broadleaf vegetation type makes the largest contribution to this remaining non-zero NEE, as its fluxes are slower to equilibrate than most other vegetation types (Fig. 6a). Broadleaf deciduous vegetation also stands out, showing a relatively large positive NEE in each 100 year period with only a slow decrease over time but typically 0.04 $\mathrm{Pg\,C\,yr^{-1}}$ of this is due to poorly conserving tiles. The tundra vegetation type gives negative NEE, getting closer to zero over time. ~~Early test simulations showed some problems with soil nitrogen getting too low, which was particularly evident for the tundra vegetation type; tundra~~ This vegetation type was found to be particularly susceptible to a poor initial choice of pool sizes, which impeded the spin-up to equilibrium due to excessive loss of soil nutrients, particularly phosphorus. Tundra pools are still recovering in the first 500 years of this simulation. Evergreen needleleaf vegetation shows little trend in NEE but some variability between 100 year periods. Other vegetation types (not shown) are generally close to zero NEE after the first 100 years.

The slightly positive NEE flux to the atmosphere is balanced by a decrease in the total carbon across all pools (Fig. 6b), which is dominated by carbon loss from the passive soil pool (which has the longest turnover time). The slow soil pool and plant wood pool show much smaller differences over time, being a carbon gain and a carbon loss respectively. ~~There is a suggestion of~~ The figure shows centennial scale variability in these pools which contributes to the decadal to centennial scale variability seen in the total carbon and likely explains the small gain in total carbon over the last 150 years of the simulation. Around two thirds of the carbon loss in the passive soil pool can be attributed to evergreen broadleaf tiles, consistent with this type contributing the largest non-zero NEE at the end of the simulation.

The behaviour of the nitrogen pools (~~not shown~~Fig. 6c) is broadly similar to the carbon pools with nitrogen loss from the passive soil pool, again largely from the evergreen broadleaf vegetation type. This loss is offset, to a greater extent than for carbon, by increases in nitrogen in the slow soil pool, primarily for the tundra vegetation type. The trend in pools is a little different for phosphorus (Fig. 6d) with both the passive and slow soil pools growing, while the inorganic phosphorus pools are declining. The pools that are changing most are typically those with the longest residence times. As for nitrogen the slow soil pool change is dominated by the tundra vegetation type but the other pool changes are split more evenly across a range of vegetation types.

4.2.3 Flux distribution and variability

The zonal mean GPP, plant and soil respiration over the last 500 years for the ProgLAI case is shown in Fig. 7a along with the GPP for the PresLAI case. The GPP distribution is broadly similar for both cases with maximum GPP in the tropics. However ProgLAI gives relatively higher GPP in the mid latitudes (40–60°) and lower GPP in the tropics than PresLAI. Plant respiration generally exceeds soil respiration in the tropics but tends to be smaller than soil respiration at mid-high latitudes.

The difference in GPP can be understood when the prognostic LAI is compared to the LAI values used in the prescribed (PresLAI) case (Fig. 7b). In the prescribed LAI case, the same LAI is used for all tiles within a grid-cell regardless of vegetation type, varying seasonally but not from year to year. Zonally averaged, the prescribed LAI is largest in the tropics, peaking at over 3.0, with annual values closer to 1.0 in the mid latitudes. In ProgLAI, the simulated LAI values are lower in the tropics than those prescribed for all vegetation types. This contrasts with the simulated LAI in the mid-latitudes when all vegetation types show as large or much larger values than those prescribed. In general the evergreen tree types show larger LAI than the other vegetation types; C4 grass is particularly low over much of its geographical range. It appears that C4 grass is more sensitive to low rainfall than co-located C3 grass, especially when CABLE is run with prognostic v_{cmax}. While C4 vegetation is annual and expected to die-back under dry conditions, CABLE does not appear capable

of re-growing the vegetation when rainfall does occur. Some improvement in the simulation might be achieved through parameter tuning, but revision of the model formulation for C4 plants may also be required.

Land carbon fluxes are highly seasonal and this is captured by the model; Fig. 8 shows NEE for the final 100 years of the simulation. In the extra-tropics NEE is positive in winter and negative in summer (driven by available radiation), while in the tropics the NEE seasonality follows precipitation, with carbon uptake in the wet season and release in the dry season. With the exception of the southern extratropics, the NEE seasonality is smaller in magnitude for the ProgLAI case than for the PresLAI case. In the northern extratropics ProgLAI shows a longer growing season but with less uptake in June and July, while positive fluxes in winter are similar to the PresLAI case. In the tropics both carbon uptake and release are smaller for ProgLAI, reflecting the lower simulated LAI in the tropics. In the southern extratropics, the larger NEE seasonality in ProgLAI will not have a large impact on the total carbon flux to the atmosphere since the southern extratropical land area is very small.

Including prognostic LAI in the simulation changes the interannual variability (IAV) of the land carbon fluxes. For global fluxes (Table 2), the standard deviation of annual GPP in the ProgLAI case is 60 % larger than in the PresLAI case. Variability in the respiration fluxes is also larger for ProgLAI, particularly for the leaf respiration. However, for global NEE the ProgLAI case gives slightly smaller standard deviation than PresLAI because GPP and leaf respiration are strongly positively correlated in the ProgLAI case, driven by the interannual variations in LAI. In the PresLAI case, with fixed LAI from year to year, the relatively small interannual variability in leaf respiration appears to be most strongly driven by temperature and has a moderate negative correlation with interannual variations in GPP. Although the IAV of global NEE is smaller for ProgLAI than PresLAI, ProgLAI shows generally larger standard deviation of NEE at mid-high latitudes than PresLAI (Fig. 9a and b). Also shown in Fig. 9c and d is the autocorrelation of NEE for 1 year lag. This shows larger positive correlation for ProgLAI than PresLAI, with the large correlations located mainly in semi-arid regions. Larger correlations for ProgLAI are expected; a year of large GPP and consequently more carbon uptake will lead to increased LAI and a tendency to maintaining large GPP

and carbon uptake in the following year. The location of the larger correlations suggests this process is most important for regions where the vegetation is more marginal.

The impact of climate variability on NEE is seen in Fig. 10 which shows the correlation between NEE and precipitation or screen-level temperature for the ProgLAI case. The correlations are similar in pattern for PresLAI and generally slightly stronger than for ProgLAI (suggesting that in ProgLAI the IAV driven by climate is slightly moderated by the autocorrelation in NEE generated by LAI variability). There are strong negative correlations with precipitation in regions where the rainfall is generally lower and plant growth is water-limited, such as at the margins of deserts. In the northern high latitudes the correlation with precipitation becomes positive. With water limitation unlikely in this region, low precipitation is likely associated with less cloud and more sunshine leading to greater photosynthesis and more negative NEE. The NEE correlation with temperature is positive almost everywhere and largest in the tropics. This is presumably due to the temperature dependence of respiration. Ciais et al. (2013, Fig. 6.17) presents the sensitivity of interannual variations in global land carbon sink to interannual variations in global land temperature and precipitation for 1980-2009, showing a large range of sensitivities across models. While not directly comparable, sensitivities calculated from the ProgLAI simulation are mostly within the range of other models but also seem quite sensitive to the time period over which the calculation is performed.

4.3 Ocean carbon

4.3.1 Temporal evolution and the global air–sea carbon flux

By design WOMBAT conserves the biogeochemical tracers in the ocean, which means the rate of change in the total carbon in the ocean and sediment pools equals the net sea–air flux~~, noting that the sea–air flux is negative for into the ocean, consistent with land fluxes (NEE)~~. The temporal evolution of the global sea–air flux of carbon ~~in the~~ for the last 100 years of the ESM simulations is shown in Fig. 11a. Over the simulation period there is a net flux of carbon out of the ocean, which is declining as the ocean slowly equilibrates with the

atmosphere. By the end of the simulation, the net outgassing of carbon from the ocean is about ~~0.6~~0.55 Pg C yr^{-1}. ~~As the~~ The net sea-air flux is declining but to reach zero will take several thousands of years. For comparison, Seferian et al. (2015) showed the drift in one CMIP5 model (see Figure 2 in Seferian et al. (2015)) where the magnitude of the modeled sea-air imbalance is similar to our simulation (0.6 Pg C yr^{-1}).

As the carbon equilibration time is set by the millennium time-scale of deep water circulation, existing computational resources are insufficient to allow the ESM simulation to reach full carbon equilibrium ($\sim$ 4000 years). We explored using the ocean initial state from a long simulation of an ocean-only simulation driven by climatological atmospheric re-analysis fields. ~~However, our ESM climate~~ This failed to reduce the drift because the climate of ACCESS-ESM1 was substantially different from the atmospheric re-analysis fields and ~~this simulation, displaying a large drift in the simulated carbon flux~~hence the ocean circulation differed significantly from the ocean-only simulation.

Within WOMBAT, if particulate organic matter and calcium carbonate are not remineralized before reaching the seafloor they can accumulate in the sediments. ~~Our simulations show that the~~ We implemented this simple sediment pool to handle high flux events and reduce the possibility of numerical instabilities. The ESM simulation showed that the global organic and inorganic carbon in the sediments are stable and small (Fig. 11b) ~~relative~~ compared to the total amount of carbon dissolved in seawater ($\approx$ 37 000 Pg C; Ciais et al., 2013). Therefore, ~~it is only the~~ in the ESM simulation the net sea–air flux of carbon ~~that alters the total amount of~~ equals the total change in carbon dissolved in the ocean~~in our simulations.~~ .

While there is a slow decline in the global mean sea–air carbon flux, the upper ocean dynamics have largely stabilised as shown by no trend in the simulated annual mean primary productivity (Fig. 11c) ~~, with an end~~ and no discernable trends in global surface DIC and alkalinity concentrations (Fig. 11d and e). Over the last 100 years of the simulation ~~value of around~~ the annual mean primary productivity is about 51 $\pm$ 1 Pg C yr^{-1}. ~~This~~ The value is consistent with global estimates of primary productivity~~of~~, which range between 45–50 Pg C yr^{-1} (e.g. Carr et al., 2006).

4.3.2 Surface field ~~Assessment~~assessment

To assess our ocean carbon cycle simulation ~~and CMIP5 simulations (Taylor et al., 2012) against observations ,~~ against observations we use a Taylor diagram (Taylor, 2001). ~~This~~ We also apply the same analysis to archived CMIP5 simulations (Taylor et al., 2012) to benchmark the performance of ACCESS-ESM relative to other CMIP5 models. A Taylor diagram allows us to summarise the bias, relative variability and correlations of the simulations with the observations. Figure 12 shows the Taylor diagram comparing the annual mean surface ~~nitrate~~phosphate, oxygen, alkalinity, DIC, temperature and salinity fields. Overlain on this plot are ~~also~~ the median values from CMIP5 assessed against observations. ~~The radial distance is the spatial~~ In the plot, the radial distance of a given simulation from the origin gives the standard deviation of the ~~ACCESS-ESM1 simulation or the CMIP5 median, normalized~~ simulation normalised by the standard deviation of the observations. The angle from the x axis ~~shows~~ provides the spatial correlation coefficient between the ~~model (and CMIP5), and the~~ simulations and the observations. The radial distance from the point marked observations gives a measure of the RMS difference between the simulation and observations normalised by the standard deviation of the observations. The ~~colours represent the~~ point's colour represents the bias in the simulation given as the relative difference in the globally averaged values between ~~our simulation (and CMIP5) and~~ simulation and observations calculated as (mean_model – mean_~~reference~~observations)/mean_~~reference~~observations; positive values ~~suggest that~~ show the model is overestimating the ~~observations and negative values, underestimating~~observed value. The observations for ~~nitrate~~phosphate, temperature and salinity come from the World Ocean Atlas climatology (WOA2005; Garcia et al., 2006a, b), while pre-industrial DIC and alkalinity are from GLODAP (Key et al., 2004). The individual CMIP5 models used to calculate the multi-model median fields, are: CanESM2, GFDL-ESM2M, HadGEM2-CC, HadGEM2-ES, IPSL-CM5A-LR, IPSL-CM5A-MR, IPSL-CM5B-LR, MPI-ESM-LR, MPI-ESM-MR (Anav et al., 2013). ~~In this paper we only used the first ensemble member of each CMIP5 model.~~ Furthermore, only the surface fields

are assessed because by the last century of the ACCESS-ESM1 simulation they show no significant drift.

~~Encouragingly all variables from~~ For all variables considered, the ACCESS-ESM1 simulation ~~show~~ shows correlations with the observations of ~~close to~~ better than 0.6~~or better~~. SST shows ~~a very high~~ the highest correlation ($R > 0.98$) with observations ~~, in fact~~ having a better correlation and lower bias than the median of the CMIP5 models, and a very similar magnitude of variability with the observations. In contrast, ~~salinity appears to be underestimated in terms of variability and mean value when compared with the observations. However in comparison with the~~ sea surface salinity (SSS) shows the lowest correlation in both ACCESS-ESM1 and CMIP5 median. ACCESS-ESM1 underestimates the observed SSS variability and has a global mean value that is less than observed. The median of the CMIP5 models ~~we see better correlation and smaller biases. These biases are perhaps unsurprising given~~ has a slightly lower correlation with the observations but with greater variability and a greater underestimate of the global averaged SSS than ACCESS-ESM1. Biases in SSS are not surprising given the challenges with capturing well the hydrological cycle in ESMs (Trenberth et al., 2003).

The poor representation of salinity in ~~our simulations (and~~ ACCESS-ESM1 and the CMIP5 ~~) translates to a poor representation of ALK, and accounts for the majority of the bias. While we could~~ simulations will impact the simulated alkalinity. ACCESS-ESM1 has large regional biases in surface salinity (Bi et al., 2013b, Fig. 16), which produce surface alkalinity biases because alkalinity is strongly influenced by air–sea freshwater exchanges. The ACCESS-ESM1 alkalinity has a similar correlation with the observations as SSS but with a weak negative bias. To reduce the alkalinity bias ~~by altering~~ of ACCESS-ESM1 one needs to reduce the export of calcium carbonate from the upper ocean~~, reducing the salinity bias would be a more effective way of improving alkalinity~~. However, given the strong relationship between SSS and surface alkalinity the higher correlation of alkalinity in the CMIP5 median with the observations suggests these models may be over-tuning their simulation to compensate for the errors in the SSS simulation.

~~DIC in~~ For DIC, ACCESS-ESM1 shows a good correlation with observations (Fig. 12), ~~comparable with~~ which is comparable with the CMIP5 median, but overestimates the magnitude of the variability when compared with CMIP5 and observations. The underestimation of the mean value, also seen in the CMIP5 ~~, may be related to the alkalinity bias enhancing the outgassing of carbon from the upper ocean relative to the observations~~median, can be attributed to the negative alkalinity bias reducing the surface DIC concentration that would be in equilibrium with the atmosphere. In comparison to the observations and CMIP5, ~~nitrate~~ phosphate is poorly represented in ACCESS-ESM1 with a large overestimation ~~. This overestimation is much larger than~~ of the surface concentration. In contrast, the median from CMIP5 ~~which conversely~~ underestimates the observed mean value. Despite a poor representation of ~~nitrate~~phosphate, this does not translate ~~to significant biases in~~ into a significant bias in global primary productivity. ~~This suggests that this excess nitrate in the surface ocean is occurring in regions where nutrients are already replete. These larger values in nitrate may be related to the export of particulate organic carbon~~However, the consequence of the poor spatial distribution of phosphate will be discussed in the next section.

While assessing the simulated values with the median CMIP5 values provides valuable insight, it does not allow us to assess the skill of our model ~~when~~ compared with individual CMIP5 models. To ~~this end the simulated state variables of the carbon system,~~ do this the simulated surface DIC and ALK values are compared with individual CMIP5 models (Fig. 13). For ALK (Fig. 13a), ACCESS-ESM1 shows a similar correlation as the CMIP5 models. The CMIP5 models range between under and over-estimating the surface alkalinity concentration. While the ACCESS-ESM1 has a negative bias in surface alkalinity it is still within the range of the CMIP5 models. For DIC, we see that our simulation sits in the middle of the CMIP5 correlation values ~~but shows the best estimate of the magnitude of the variability.The DIC biases in the~~ with the lowest RMS error with the observations (Fig. 13b). All simulations show negative DIC biases and ACCESS-ESM1 is not a significant outlier. Overall, our simulation has comparable skill to the existing CMIP5 models~~show a large range, that both under and overestimate the mean value. Our simulation , which~~

underestimates the mean value, is comparable in magnitude to those models that also underestimate the mean value. The simulated ALK (Fig. 13b) shows a similar correlation as the CMIP5 models, but shows a larger variability than most, at the top end of the CMIP5 range. All CMIP5 models underestimate the mean ALK value .

4.3.3 BGC fields

The Taylor diagrams provide a useful quantitative assessment of model simulations but a visual comparison of the key BGC fields provides important spatial context to the model - observation assessment. To start the comparison with observations, we first look at the ACCESS-ESM1 simulation of Net Primary Productivity (NPP), surface phosphate, export production from 100m and sea-air CO_2 fluxes from the last 100 years of the simulation (Fig. 14). In this comparison, we have also included the ACCESS ocean-only simulation forced by the CORE seasonal mean forcing (Large and Yeager, 2004), with the same ocean carbon parameters as ACCESS-ESM1, to evaluate how biases in the climate model impact the ocean carbon cycle. The observed estimates of NPP are based on using the chlorophyll derived from the seasonal SeaWiFS climatology and the Eppley-VGPM algorithm. The algorithm employs the basic model structure and parameterization of the standard VGPM (Behrenfeld and Falkowski, 1997) but replaces the polynomial description of Pb_{opt} with the exponential relationship described by Morel (1991) and based on the curvature of the temperature-dependent growth function described by Eppley (1972). The annual sea-air fluxes of CO_2 are based on Takahashi et al. (2009). The observations for phosphate come from the World Ocean Atlas climatology (WOA2005; Garcia et al., 2006a).

The ACCESS-ESM1 simulation of NPP is poor with too much production in the western tropical Indian and Pacific oceans and too little NPP in the high latitude oceans (Fig. 14a). The excessive NPP in the tropics and under-estimated NPP in the high latitudes is exacerbated in the ACCESS-ESM1 simulation compared to the observations; our simulationgives a larger underestimation than most models, but is within the range of CMIP5. As discussed earlier this bias is likely related to our bias in surface salinity, and appears to be a common feature of these simulations. Overall, our simulation has

~~comparable skill to the existing CMIP5 models.~~ ocean-only simulation, revealing that biases in the climate simulation significantly degrade NPP. The excessive tropical Pacific NPP reflects the strong cold tongue bias in the ACCESS-ESM1 simulation, which upwells too much phosphate in the tropical Pacific and elevates phosphate in the western tropical Pacific particularly. Outside of the tropics NPP from the ocean-only simulation is generally slightly less than the observations and NPP further declines in the ESM simulation. Changes in NPP between the ESM simulation and the ocean-only simulation reflect biases in the circulation and enhance recycling of phosphate in the upper ocean. The enhanced recycling of phosphate in the ACCESS-ESM1 simulations is revealed by greater tropical NPP but less export production through 100 m (Fig. 14b). The enhanced recycling of nutrients further helps to increase the phosphate concentration in the surface and to degrade the phosphate simulation as revealed in the Taylor diagram (Fig. 14c).

4.3.4 ~~Sea-air carbon flux variability~~

NPP shows much greater difference between the ESM and ocean-only simulation than net sea-air flux (Fig. 14d). The similarity suggests the sea-air fluxes are not too sensitive to the NPP biases of the ESM simulation because most of the changes in the ESM simulation reflected increased nutrient recycling rather than increased carbon export out of the upper ocean. The sea–air carbon flux ~~is shown in Fig. 14~~ for the last century of the ESM simulation (901–1000) ~~. The simulations show~~ shows outgassing in the tropical ocean and in the Southern Ocean and uptake in the Southern and Northern Hemispheres mid-latitudes. This spatial pattern of the sea–air fluxes is in ~~very good~~ agreement with the integrated pre-industrial zonal sea–air fluxes estimated by Gruber et al. (2009) and similar to the present day flux climatology of Takahashi et al. (2009), which includes the anthropogenic increase atmospheric CO_2.

Zonally-averaged sections of phosphate, oxygen, DIC and alkalinity concentrations are compared to observations to help further elucidate the limitations in the ACCESS-ESM1 simulation (Fig. 15). The observations for phosphate come from the World Ocean Atlas

climatology (WOA2005; Garcia et al., 2006a), while pre-industrial DIC and alkalinity are from GLODAP (Key et al., 2004).

Consistent with the Taylor diagram analysis the simulated DIC values are too low throughout the ocean, in part because the low surface alkalinity lowers pCO_2 in the surface and retards the solubility uptake of CO_2 (Fig. 15a). For alkalinity, the simulated values are too low at the surface with a too strong vertical gradient (Fig. 15b). Reducing the export of calcium carbonate would help improve the simulated alkalinity by raising surface alkalinity and reducing alkalinity in the ocean interior.

The phosphate section shows the simulated deep water concentrations slightly less than observed with a big positive bias in the simulation confined to the upper 1000 m of the ocean (Fig. 15c). Deepening the remineralization of sinking detritus would be one way to transfer the excessive phosphate from the upper ocean into the deep ocean. The deepening of detritus remineralization would help reduce the simulated excessive oxygen concentrations and raise the DIC concentrations in the deep ocean and make the simulation more consistent with the observations (Fig. 15a and d).

While more effort is required to tune the ocean BGC parameters to increase the depth of detritus remineralization and reduce calcium carbonate export, the ACCESS-ESM1 overall behaviour of the surface BGC fields is not significantly worse than other CMIP5 simulations. However the biases in the ACCESS-ESM1 simulation will need to be considered when interpreting how the model responds to historical and future atmospheric CO_2 levels. ~~The interannual variability (1 sigma)was computed by removing the seasonal monthly climatology , calculated from the last century of the simulation, from the monthly fluxes. The resulting fluxes were then averaged into annual fluxes from which the standard deviation in the variability was determined. Regions of high variability include the tropical Pacific, the North Atlantic and the upwelling regions of Java, Arabia, South America and Africa. There is also a band of elevated variability in the Southern Ocean but it is significantly less than the high variability areas in the tropics.~~

5 Conclusion and future model development

~~Documentation~~ The key components and features of ACCESS-ESM1 ~~and its performance under pre-industrial, prescribed atmospheric~~ have been described. CABLE simulates land carbon fluxes and pools, with the capability of accounting for nitrogen and phosphorus limitation. Leaf area index can be simulated, although phenology is prescribed. Inputs to the land carbon system e.g. nitrogen fixation are fixed and there is also no change in vegetation distribution. Thus we do not account for land use change over the historical period. WOMBAT simulates ocean carbon biogeochemistry of DIC, Alkalinity, phosphate, iron and oxygen with single phytoplankton and zooplankton compartments. The growth of the phytoplankton is limited by phosphate, iron and light and the phytoplankton produce a fixed fraction of calcium carbon to organic carbon.

This paper has described the behaviour of ACCESS-ESM1 for the relatively simple case of pre-industrial conditions with prescribed atmospheric CO_2 ~~conditions is important for ongoing work with this model version. In this paper two~~ . A second part of this study (Ziehn et al., 2016) evaluates the model over the historical period, again with prescribed atmospheric CO_2. Two ACCESS-ESM1 simulations were compared; both used the same ocean biogeochemistry and the land carbon module with nutrient limitation (N and P) active but one used prescribed LAI and the other prognostic LAI. Simulating LAI (ProgLAI) increased interannual variability in GPP and respiration fluxes, but not in global total NEE, and also gave a slight warming of the climate. ProgLAI tended to underestimate the LAI in the tropics and overestimate LAI at high latitudes, compared to the dataset used in the prescribed LAI case. The different LAI distribution impacted the spatial distribution and seasonal cycle of carbon fluxes. Despite the apparent biases in the simulation of leaf area index (in ProgLAI), this is our preferred configuration because it is important that LAI is responsive to climate, especially for scenario simulations out to 2100. ~~Overall, the analysis presented here, and for the historical period (Ziehn et al., 2016) shows that the land carbon module provides realistic simulations of land carbon exchange.~~ For ocean carbon, we see reasonable agreement with observations, and results that fall within the range of existing

CMIP5 models for DIC and alkalinity. The spatial pattern of pre-industrial sea–air carbon fluxes shows good agreement with published studies. Global primary productivity is close to the observed value although the spatial distribution does not match observations well.

Analysis of the pre-industrial simulation has highlighted some critical issues with the ACCESS-ESM1 carbon models and how biases in the physical model simulation can contribute to a poor simulation of carbon fluxes. For land carbon, a high priority is to fix the inability of CABLE to conserve carbon in ~~situations~~ (localised) regions where moisture is insufficient to maintain vegetation~~and to confirm whether land carbon fluxes are too sensitive to climate (particularly rainfall) variability. Development priorities for CABLE in future ACCESS-ESM versions are implementation of land use change,~~ . A solution has been developed for the standalone version of CABLE, but its effectiveness in the coupled version is still being assessed. However, even when carbon conservation is resolved, the coupled system may still respond poorly in regions where the physical model significantly underestimates rainfall and carbon pools become depleted. This was particularly noticeable for the C4 grass vegetation type. Work being undertaken with the ~~ability for phenology to respond to climate and improved nutrient forcing (e. g. temporally varying input fluxes).~~

~~In the ocean we see reasonable agreement with observations, and results that fall within the range of existing CMIP5 models for DIC and alkalinity. The spatial pattern of pre-industrial sea–air carbon fluxes shows very good agreement with published studies, while primary productivity is close to the observed value. Nevertheless there are~~ standalone version of CABLE to allow the phenology of grasses to be soil moisture and temperature dependent (V. Haverd, pers. comm.) may help to improve this aspect of the simulation. Key outstanding issues to be addressed in the ocean are: (a) reducing surface salinity biases would improve the simulated values of alkalinity and DIC, bringing ~~these~~ them closer to the observations; ~~and~~ (b) reducing the excess of surface ~~nitrate~~phosphate, potentially through modifying the particulate organic carbon export~~. Furthermore we see a recognised need to add additional complexity, in terms of phytoplankton and zooplankton classes, to capture the potential impacts related to projected changes in the marine environment~~

such as ocean acidification (e.g. Matear and Lenton, 2014); and (c) reducing the export of calcium carbonate to improve interior alkalinity concentrations.

It is clear from our simulations that our model has yet to fully reach quasi-steady state, despite more than 1000 years of simulation. , with a global sea-air flux still greater than 0.55 $PgC\,yr^{-1}$. This slow equilibration, along with the localised land carbon non-conservation, means that ACCESS-ESM1 is not yet suitable for running emissions-driven simulations, unless a carbon flux correction is applied. Prescribed atmospheric CO_2 simulations remain useful and analysis is being undertaken of a range of representative concentration pathway (RCP) simulations out to 2100.

At present, computational limitations inhibit our ability to optimise the model behaviour and produce carbon fields that are equilibrated with the pre-industrial atmosphere. Therefore in the longer term, we need to develop better ways to tune the carbon models and accelerate the convergence of both the land and ocean carbon models to steady state (e.g. Fang et al., 2015). We also need to work closely with those developing the physical model components of ACCESS, since the quality of the carbon simulation is dependent on the quality of the physical model simulation.

Development priorities for CABLE in future ACCESS-ESM versions are implementation of land use change, the ability for phenology to respond to climate and improved nutrient forcing (e.g. temporally varying input fluxes). For WOMBAT, we see a recognised need to add additional complexity, in terms of phytoplankton and zooplankton classes, to capture the potential impacts related to projected changes in the marine environment such as ocean acidification (e.g. Matear and Lenton, 2014).

At present the next physical model version of ACCESS (ACCESS-CM2) is currently being developed in preparation for CMIP6. The land and ocean carbon cycles presented here will form the basis for ACCESS-ESM2, once we have resolved the critical deficiencies that this study has elucidated.

Appendix A: ACCESS1.4 compared to ACCESS1.3

Details of model code differences between the published ACCESS1.3 version (Bi et al., 2013b) and the physical model version used here (ACCESS1.4) are noted for each model component (Fig. 1). The impact of these changes on the pre-industrial climate model simulation is also noted.

A1 Atmosphere component

ACCESS1.3 used atmospheric physics settings similar to the Met Office Global Atmosphere (GA) 1.0 configuration (Hewitt et al., 2011) including the "PC2" cloud scheme (Wilson et al., 2008). A similar configuration is used for ACCESS1.4.

Analysis of ACCESS1.3 simulations showed almost no dust in the atmosphere (Dix et al., 2013); this was a consequence of changing the land surface scheme from the original UM land scheme to CABLE and freezing the ACCESS1.3 code version for CMIP5 before finalising dust settings. As described in Dix et al. (2013), the dust-uplift scheme used in the ACCESS models is based on Woodward (2001) and Woodward (2011), with dust being modelled for nine size bins with different particle diameters. Dust uplift can occur over bare soil and depends on wind speed, soil composition and volumetric soil-moisture content in the surface layer. Dust-uplift settings used by ACCESS1.4 for the tuneable parameters described in Woodward (2011) are friction-velocity tuneable constant $k_1 = 1.6$, soil-moisture tuneable constant $k_2 = 0.5$, overall scaling factor $C = 6.525$, maximum clay fraction for dust emissions of 0.1 and no preferential source term. These settings result in a global annual mean dust burden of 14.9 ± 1.3 Tg (calculated over 160 years from an ACCESS1.4 pre-industrial control simulation), which is broadly comparable to the AEROCOM multi-model median value of 15.8 Tg for year 2000 conditions (Huneeus et al., 2011).

In addition to the change in dust, the ACCESS1.3 control simulation did not include background stratospheric volcanic forcing but this has been included in ACCESS1.4 simulations. Preliminary tests with the dust and vocanic forcing changes reduced the globally averaged surface air temperature relative to ACCESS1.3. Since an aim of ACCESS1.4 was not to change global-scale climate characteristics relative to ACCESS1.3,

one of the parameters in the cloud scheme (FW_STD associated with the standard deviation of cloud water content) was increased from 0.700 in ACCESS1.3 to 0.725 in ACCESS1.4. This resulted in a globally averaged surface air temperature in ACCESS1.4 that was similar to that obtained for ACCESS1.3. ACCESS1.4 also corrects a bug which zeroed the downward short-wave radiation over coastal sea-ice points for non-radiation timesteps. This reduced excess ice accumulation in ACCESS1.3 in some coastal regions such as the Canadian Archipelagos.

A2 Land component

CABLE was implemented in ACCESS1.3 at version 1.8 (CABLE1.8, (Kowalczyk et al., 2013)) while ACCESS1.4 uses CABLE2.2.3. CABLE2.2.3 has a number of small science changes and bug fixes from CABLE1.8. These dealt with occasional non-physical exchange coefficients, addressed some poor behaviour under very dry conditions, improved the water balance in the coupled system and ensured all CABLE variables were correctly being passed back into the ACCESS atmosphere e.g. for use by dry deposition. CABLE in ACCESS1.3 used a constant (370 ppm) (internal to CABLE) atmospheric CO_2 for all simulations while ACCESS1.4 correctly passes the atmospheric CO_2 from the UM to CABLE. Often these changes could be shown to improve CABLE's performance in standalone mode for individual locations (e.g. at desert sites for the dry condition changes) but did not have broad-scale impacts when tested globally in atmosphere-only ACCESS simulations. Thus the assessment of the land surface impacts on the ACCESS climate for ACCESS1.3 (Kowalczyk et al., 2013) would also be applicable to ACCESS1.4 simulations. The improvements to the water balance approximately halved the drift in global ocean salinity in ACCESS1.4 compared to ACCESS1.3.

A3 Ocean component

While there are no changes in the ocean model version between ACCESS1.3 and ACCESS1.4, there have been two changes in the configuration or parameter values.

Firstly for ACCESS1.4, the background vertical diffusivity outside 20° S to 20° N has been increased from 0.5×10^{-5} to 1.0×10^{-5} $m^2\,s^{-1}$, which is also consistent with the value used in ACCESS-OM. Secondly, the ocean absorption of penetrative solar radiation is now calculated using the diffuse attenuation coefficient of the downwelling photosynthetically available radiation (K_{dPAR}) rather than the downwelling spectral irradiance at wavelength 490 nm (K_{d490}). Since K_{dPAR} data covers a broader, more representative, spectrum of light, it is considered to be more appropriate for use in the ocean model and was also the dataset used in the standard ACCESS-OM configuration. Bi et al. (2013a) compares ACCESS-OM simulations using K_{dPAR} and K_{d490} and concludes that differences are mostly confined to the subsurface water between 40° S to 40° N with little impact on the deep ocean climate or the global ocean circulation and associated water volume transports.

A4 OASIS coupler

ACCESS1.3 used the OASIS3.2-5 coupler (Valcke, 2006). In ACCESS1.4, this is replaced by OASIS3-MCT (Valcke et al., 2013) which is designed to provide more efficient coupling for models running on many processors. For ACCESS1.4, this enables the simulation of about 7.2 model years per day (using 144 processors) compared to 5.4 model years per day for ACCESS1.3.

A5 Comparison of pre-industrial climate across ACCESS versions

The two ACCESS submissions to CMIP5, ACCESS1.0 and ACCESS1.3 produced similar results, relative to the range of CMIP5 models, when various modelled atmospheric climate variables were compared against observations (e.g. Flato et al., 2013, Fig. 9.7). Here we show that ACCESS1.4 (and ACCESS-ESM1) simulations are more similar to ACCESS1.3 than ACCESS1.0 was to ACCESS1.3. We use monthly mean values averaged across 100 years from pre-industrial climate simulations and and calculate the root mean square difference (RMSD), similar to Gleckler et al. (2008), between each modelled field (F) and that modelled by ACCESS1.3 (R). The RMSD is calculated across all longitude (i) and

latitude (j) and, depending on the variable, at different pressure levels:

$$\mathrm{RMSD}^2 = \frac{1}{W}\sum_i\sum_j\sum_t w_{ijt}(F_{ijt} - R_{ijt})^2 \quad \text{(A1)}$$

where t corresponds to the time dimension (12 months) and W is the sum of the weights (w_{ijt}) which, for the spatial domain, are proportional to the grid-cell area. We then normalise by the ACCESS1.0 RMSD:

$$\mathrm{RMSD}_{\mathrm{norm}} = \mathrm{RMSD}_{\mathrm{model}}/\mathrm{RMSD}_{\mathrm{ACCESS1.0}} \quad \text{(A2)}$$

such that a value of 1 indicates that the simulated variable is as different from ACCESS1.3 as ACCESS1.0 is from ACCESS1.3 while values smaller than 1 indicate a simulation that is closer to that of ACCESS1.3.

Figure 16 shows that for a range of atmospheric variables the normalised RMSD for ACCESS1.4 is generally around 0.3–0.4 indicating that the ACCESS1.4 climate simulation is much closer to ACCESS1.3 than ACCESS1.0 is to ACCESS1.3. This would be expected given the relatively small number of science changes between ACCESS1.3 and ACCESS1.4. Likewise the ACCESS-ESM1 simulation with prescribed LAI shows similar RMS differences from ACCESS1.3, implying little or no change from the ACCESS1.4 simulation when the carbon cycle is included but the atmospheric CO_2 is prescribed. The RMS differences for ACCESS-ESM1 with prognostic LAI are generally similar or slightly larger than for the case with prescribed LAI, with the largest differences being for near surface and lower tropospheric temperature and geopotential height at 500 hPa.

Code availability

Code availability varies for different components of ACCESS-ESM1. The UM is licensed by the UK Met Office and is not freely available. CABLE2 is available from https://trac.nci.org.au/svn/cable/ following registration. See https://trac.nci.org.au/trac/cable/wiki/

CableRegistration for information on registering to use the CABLE repository. MOM4p1 and CICE are freely available under applicable registration or copyright conditions. For MOM4p1 see https://github.com/BreakawayLabs/MOM4p1. For CICE see http://oceans11.lanl.gov/trac/CICE. For access to the MOM4p1 code with WOMBAT as used for ACCESS-ESM1, please contact Hailin Yan (Hailin.Yan@csiro.au). The OASIS3-MCT 2.0 coupler code is available from http://oasis.enes.org.

The Supplement related to this article is available online at doi:10.5194/gmdd-0-1-2016-supplement.

Acknowledgements. This research is supported by the Australian Government Department of the Environment, the Bureau of Meteorology and CSIRO through the Australian Climate Change Science Programme. The research was undertaken on the NCI National Facility in Canberra, Australia, which is supported by the Australian Commonwealth Government. The authors wish to acknowledge use of the Ferret program for some of the analysis and graphics in this paper. Ferret is a product of NOAA's Pacific Marine Environmental Laboratory. (Information is available at http://ferret.pmel.noaa.gov/Ferret/). Ashok Luhar provided helpful feedback on the manuscript. Mark Collier implemented the PCDMI metrics package, which was used for the comparison of atmospheric variables between ACCESS model versions. Arnold Sullivan helped produce some of the figures.

References

Anav, A., Friedlingstein, P., Kidston, M., Bopp, L., Ciais, P., Cox, P., Jones, C., Jung, M., Myneni, R., and Zhu, Z.: Evaluating the land and ocean components of the global carbon cycle in the CMIP5 Earth System Models, J. Climate, 26, 6801–6843, 2013.

Anderson, L. A. and Sarmiento, J. L.: Redfield ratios of remineralization determined by nutrient data analysis, Global Biogeochem. Cy., 8, 65–80, 1994.

Arora, V. K., Boer, G. J., Friedlingstein, P., Eby, M., Jones, C. D., Christian, J. R., Bonan, G., Bopp, L., Brovkin, V., Cadule, P., Hajima, T., Ilyina, T., Lindsay, K., Tjiputra, J. F., and Wu, T.:

Carbon-concentration and carbon-climate feedbacks in CMIP5 Earth System Models, J. Climate, 26, 5289–5314, 2013.

Behrenfeld, M. J. and Falkowski, P. G.: Photosynthetic rates derived from satellite-based chlorophyll concentration, Limnology and Oceanography, 42, 1–20, 1997.

Bi, D., Marsland, S. J., Uotila, P., O'Farrell, S., Fiedler, R., Sullivan, A., Griffies, S. M., Zhou, X., and Hirst, A. C.: ACCESS-OM: the ocean and sea-ice core of the ACCESS coupled model, Aust. Meteor. Oceanogr. J., 63, 213–232, 2013a.

Bi, D., Dix, M., Marsland, S. J., O'Farrell, S., Rashid, H. A., Uotila, P., Hirst, A. C., Kowalczyk, E., Golebiewski, M., Sullivan, A., Yan, H., Hannah, N., Franklin, C., Sun, Z., Vohralik, P., Watterson, I., Zhou, X., Fiedler, R., Collier, M., Ma, Y., Noonan, J., Stevens, L., Uhe, P., Zhu, H., Griffies, S. M., Hill, R., Harris, C., and Puri, K.: The ACCESS coupled model: description, control climate and evaluation, Aust. Meteor. Oceanogr. J., 63, 41–64, 2013b.

Boer, G. J. and Arora, V. K.: Feedbacks in emission-driven and concentration-driven global carbon budgets, J. Climate, 26, 3326–3314, doi:10.1175/JCLI-D-12-00365.1, 2012.

Boyer, T. P., Antonov, J. I., Baranova, O. K., Garcia, H. E., Johnson, D. R., Locarnini, R. A., Mishonov, A. V., O'Brien, T., Seidov, D., and Smolyar, I. V.: World Ocean Database 2009, Vol. 66, NOAA Atlas NESDIS, US Gov. Printing Office, Wash., D.C., available at: http://www.vliz.be/imis/imis.php?module=ref&refid=205411 (last access: 16 September 2015), 2009.

Carr, M.-E., Friedrichs, M. A. M., Schmeltz, M., Aita, M. N., Antoine, D., Arrigo, K. R., Asanuma, I., Aumont, O., Barber, R., Behrenfeld, M., Bidigare, R., Buitenhuis, E., Campbell, J., Ciotti, A., Dierssen, H., Dowell, M., Dunne, J., Esaias, W., Gentili, B., Gregg, W., Groom, S., Hoepffner, N., Ishizaka, J., Kameda, T., Le Quéré, C., Lohrenz, S., Marra, J., Mélin, F., Moore, J., Morel, A., Reddy, T. E., Ryan, J., Scardi, M., Smyth, T., Turpie, K., Tilstone, G., Waters, K., and Yamanaka, Y.: A comparison of global estimates of marine primary production from ocean color, Deep-Sea Res. Pt. II, 53, 741–770, 2006.

Ciais, P., Sabine, C., Bala, G., Bopp, L., Brovkin, V., Canadell, J., Chhabra, A., DeFries, R., Galloway, J., Heimann, M., Jobes, C., Le Quéré, C., Myneni, R. B., Piao, S., and Thornton, P.: Carbon and other biogeochemical cycles, in: Climate Change 2013: The Physical Science Basis. Contribution of Working Group I to the Fifth Assessment Report of the Intergovernmental Panel on Climate Change, edited by: Stocker, T. F., Qin, D., Plattner, G.-K., Tignor, M., Allen, S. K., Boschung, J., Nauels, A., Xia, Y., Bex, V., and Midgley, P. M., Cambridge University Press, Cambridge, UK and New York, NY, USA, 465–570, 2013.

Comiso, J.: updated 2012. *Bootstrap Sea Ice Concentrations from Nimbus-7 SMMR and DMSP SSM/I-SSMIS.* Version 2. [1978 - 2007], National Snow and Ice Data Center, 2000.

Cox, P. D., Betts, R. A., Jones, C. D., Spall, S. A., and Totterdell, I. J.: Acceleration of global warming due to carbon-cycle feedbacks in a coupled climate model, Nature, 408, 184–187, 2000.

Dix, M., Vohralik, P., Bi, D., Rashid, H., Marsland, S., O'Farrell, S., Uotila, P., Hirst, T., Kowalczyk, E., Sullivan, A., Yan, H., Franklin, C., Sun, Z., Watterson, I., Collier, M., Noonan, J., Rotstayn, L., Stevens, L., Uhe, P., and Puri, K.: The ACCESS coupled model: documentation of core CMIP5 simulations and initial results, Aust. Meteor. Oceanogr. J., 63, 83–99, 2013.

Eppley, R. W.: Temperature and phytoplankton growth in the sea, Fish. Bull. U.S., 70, 1063–1085, 1972.

Exbrayat, J.-F., Pitman, A. J., Abramowitz, G., and Wang, Y.-P.: Sensitivity of net ecosystem exchange and heterotrophic respiration to parameterization uncertainty, J. Geophys. Res.-Atmos., 118, 1–12, doi:10.1029/2012JD018122, 2013.

Fang, Y., Liu, C., and Leung, L. R.: Accelerating the spin-up of the coupled carbon and nitrogen cycle model in CLM4, Geosci. Model Dev., 8, 781–789, doi:10.5194/gmd-8-781-2015, 2015.

Flato, G., Marotzke, J., Abiodun, B., Braconnot, P., Chou, S., Collins, W., Cox, P., Driouech, F., Emori, S., Eyring, V., Forest, C., Gleckler, P., Guilyardi, E., Jakob, C., Kattsov, V., Reason, C., and Rummukainen, M.: Evaluation of Climate Models, in: Climate Change 2013: The Physical Science Basis. Contribution of Working Group I to the Fifth Assessment Report of the Intergovernmental Panel on Climate Change, edited by: Stocker, T. F., Qin, D., Plattner, G.-K., Tignor, M., Allen, S., Boschung, J., Nauels, A., Xia, Y., Bex, V., and Midgley, P., 741–866, Cambridge University Press, Cambridge, UK and New York, NY, USA, 2013.

Friedlingstein, P., Bopp, L., Ciais, P., Dufresne, J.-L., Fairhead, L., LeTreut, H., Monfray, P., and Orr, J.: Positive feedback between future climate change and the carbon cycle, Geophys. Res. Lett., 28, 1543–1546, 2001.

Friedlingstein, P., Cox, P., Betts, R., Bopp, L., von Bloch, W., Brovkin, V., Cadule, P., Doney, S., Eby, M., Fung, I., Bala, G., John, J., Jones, C., Joos, F., Kato, T., Kawamiya, M., Knorr, W., Lindsay, K., Matthews, H. D., Raddatz, T., Rayner, P., Reick, C., Roeckner, E., Schnitzler, K.-G., Schnur, R., Strassmann, K., Weaver, A. J., Yoshikawa, C., and Zeng, N.: Climate–carbon cycle feedback analysis: results from the C^4MIP model intercomparison, J. Climate, 19, 3337–3353, doi:10.1175/JCLI3800.1, 2006.

Friedlingstein, P., Meinshausen, M., Arora, V. K., Jones, C. D., Anav, A., Liddicoat, S. K., and Knuitti, R.: Uncertainties in CMIP5 climate projections due to carbon cycle feedbacks, J. Climate, 27, 511–526, 2014.

Garcia, H., Locarnini, R., and Boyer, T.: World ocean atlas 2005, Volume 3: Dissolved oxygen, apparent oxygen utilization, in: NOAA Atlas NESDIS 63, edited by: Levitus, S., US Government Printing Office, Washington, D.C., 342 pp., 2006a.

Garcia, H., Locarnini, R., Boyer, T., and Antonov, J.: World ocean atlas 2005, Volume 4: Nutrients (phosphate, nitrate, silicate), in: NOAA Atlas NESDIS 63, edited by: Levitus, S., US Government Printing Office, Washington, D.C., 396 pp., 2006b.

Gleckler, P. J., Taylor, K. E., and Doutriaux, C.: Performance metrics for climate models, J. Geophys. Res., 113, D06104, doi:10.1029/2007JD008972, 2008.

Griffies, S. M.: Elements of MOM4p1, GFDL Ocean Group, Tech. Rep. No. 6, NOAA/Geophysical Fluid Dynamics Laboratory, Princeton, USA, 2009.

Gruber, N., Gloor, M., Fletcher, S. E. M., Doney, S. C., Dutkiewicz, S., Follows, M. J., Gerber, M., Jacobson, A. R., Joos, F., Lindsay, K., Menemenlis, D., Mouchet, A., Muller, S. A., Sarmiento, J. L., and Takahashi, T.: Oceanic sources, sinks, and transport of atmospheric CO_2, Global Biogeochem. Cy., 23, GB1005, doi:10.1029/2008gb003349, 2009.

Hewitt, H. T., Copsey, D., Culverwell, I. D., Harris, C. M., Hill, R. S. R., Keen, A. B., McLaren, A. J., and Hunke, E. C.: Design and implementation of the infrastructure of HadGEM3: the next-generation Met Office climate modelling system, Geosci. Model Dev., 4, 223–253, doi:10.5194/gmd-4-223-2011, 2011.

Huang, M., Piao, S., Sun, Y., Ciais, P., Cheng, L., Mao, J., Poulter, B., Shi, X., Zeng, Z., and Wang, Y.: Change in terrestrial ecosystem water-use efficiency over the last three decades, Glob. Change Biol., 21, 2366–2378, doi:10.1111/gcb.12873, 2015.

Huneeus, N., Schulz, M., Balkanski, Y., Griesfeller, J., Prospero, J., Kinne, S., Bauer, S., Boucher, O., Chin, M., Dentener, F., Diehl, T., Easter, R., Fillmore, D., Ghan, S., Ginoux, P., Grini, A., Horowitz, L., Koch, D., Krol, M. C., Landing, W., Liu, X., Mahowald, N., Miller, R., Morcrette, J.-J., Myhre, G., Penner, J., Perlwitz, J., Stier, P., Takemura, T., and Zender, C. S.: Global dust model intercomparison in AeroCom phase I, Atmos. Chem. Phys., 11, 7781–7816, doi:10.5194/acp-11-7781-2011, 2011.

Hunke, E. C. and Lipscomb, W. H.: CICE: The Los Alamos sea ice model documentation and software user's manual, Version 4.1, LA-CC-06-012, Los Alamos National Laboratory, N.M., 2010.

Jones, C., Robertson, E., Arora, V., Friedlingstein, P., Shevliakova, E., Bopp, L., Brovkin, V., Hajima, T., Kato, E., Kawamiya, M., Liddicoat, S., Lindsay, K., Reick, C. H., Roelandt, C., Segschneider, J., and Tjiputra, J.: Twenty-first-century compatible CO_2 emissions and airborne fraction simulated by CMIP5 Earth System Models under four representative concentration pathways, J. Climate, 26, 4398–4413, 2013.

Jones, C. D., Hughes, J. K., Bellouin, N., Hardiman, S. C., Jones, G. S., Knight, J., Liddicoat, S., O'Connor, F. M., Andres, R. J., Bell, C., Boo, K.-O., Bozzo, A., Butchart, N., Cadule, P., Corbin, K. D., Doutriaux-Boucher, M., Friedlingstein, P., Gornall, J., Gray, L., Halloran, P. R., Hurtt, G., Ingram, W. J., Lamarque, J.-F., Law, R. M., Meinshausen, M., Osprey, S., Palin, E. J., Parsons Chini, L., Raddatz, T., Sanderson, M. G., Sellar, A. A., Schurer, A., Valdes, P., Wood, N., Woodward, S., Yoshioka, M., and Zerroukat, M.: The HadGEM2-ES implementation of CMIP5 centennial simulations, Geosci. Model Dev., 4, 543–570, doi:10.5194/gmd-4-543-2011, 2011.

Jones, P. and Harris, I.: CRU TS3.22: Climatic Research Unit (CRU) Time-Series (TS) Version 3.22 of High Resolution Gridded Data of Month-by-month Variation in Climate (Jan. 1901- Dec. 2013), doi:10.5285/18BE23F8-D252-482D-8AF9-5D6A2D40990C, http://dx.doi.org/10.5285/18BE23F8-D252-482D-8AF9-5D6A2D40990C, 2014.

Kattge, J., Knorr, W., Raddatz, T., and Wirth, C.: Quantifying photosynthetic capacity and its relationship to leaf nitrogen content for global-scale terrestrial biosphere models, Glob. Change Biol., 15, 976–991, doi:10.1111/j.1365-2486.2008.01744.x, 2009.

Kelly, R. H., Parton, W. J., Hartman, M. D., Stretch, L. K., Ojima, D. S., and Schimel, D. S.: Intra-annual and interannual variability of ecosystem processes in shortgrass steppe, J. Geophys. Res., 105, 20093–20100, doi:10.1029/2000JD900259, 2000.

Key, R. M., Kozyr, A., Sabine, C. L., Lee, K., Wanninkhof, R., Bullister, J. L., Feely, R. A., Millero, F. J., Mordy, C., and Peng, T. H.: A global ocean carbon climatology: results from Global Data Analysis Project (GLODAP), Global Biogeochem. Cy., 18, GB4031, doi:10.1029/2004GB002247, 2004.

Kowalczyk, E. A., Wang, Y. P., Law, R. M., Davies, H. L., McGregor, J. L., and Abramowitz, G.: The CSIRO Atmosphere Biosphere Land Exchange (CABLE) model for use in climate models and as an offline model, CSIRO Marine and Atmospheric Research technical paper 13, Aspendale, Victoria, Australia, 2006.

Kowalczyk, E. A., Stevens, L., Law, R. M., Dix, M., Wang, Y. P., Harman, I. N., Haynes, K., Srbinovsky, J., Pak, B., and Ziehn, T.: The land surface model component of ACCESS: description and impact on the simulated surface climatology, Aust. Meteor. Oceanogr. J., 63, 65–82, 2013.

Large, W. and Yeager, S. G.: Diurnal to decadal global forcing for ocean and Sea-Ice models: The data sets and flux climatologies, Tech. Rep. NCAR/TN-460+STR, 2004.

Lawrence, P. J., Feddema, J. J., Bonan, G. B., Meehl, G. A., O'Neill, B. C., Oleson, K. W., Levis, S., Lawrence, D. M., Kluzek, E., Lindsay, K., and Thornton, P. E.: Simulating the biogeochemical and biogeophysical impacts of transient land cover change and wood harvest in the Community Climate System Model (CCSM4) from 1850 to 2100, J. Climate, 25, 3071–3095, doi:10.1175/JCLI-D-11-00256.1, 2012.

Lenton, A. and Matear, R. J.: Role of the Southern Annular Mode (SAM) in Southern Ocean CO_2 uptake, Global Biogeochem. Cy., 21, GB2016, doi:10.1029/2006GB002714, 2007.

Marsland, S. J., Bi, D., Uotila, P., Fiedler, R., Griffies, S. M., Lorbacher, K., O'Farrell, S., Sullivan, A., Uhe, P., Zhou, X., and Hirst, A. C.: Evaluation of ACCESS climate model ocean diagnostics in CMIP5 simulations, Aust. Meteor. Oceanogr. J., 63, 101–119, 2013.

Martin, G. M., Milton, S. F., Senior, C. A., Brooks, M. E., Ineson, S., Reichler, T., and Kim, J.: Analysis and reduction of systematic errors through a Seamless approach to modelling weather and climate, J. Climate, 23, 5933–5957, doi:10.1175/2010JCLI3541.1, 2010.

Matear, R. J. and Lenton, A.: Quantifying the impact of ocean acidification on our future climate, Biogeosciences, 11, 3965–3983, doi:10.5194/bg-11-3965-2014, 2014.

Morel, A.: Light and marine photosynthesis: a spectral model with geochemical and climatological implications, Progress In Oceanography, 26, 263–306, 1991.

O'Kane, T. J., Matear, R. J., Chamberlain, M. A., and Risbey, J. S.: Decadal variability in an OGCM Southern Ocean: intrinsic modes, forced modes and metastable states, Ocean Model., 16, 1–21, doi:10.1016/j.ocemod.2013.04.009, 2013.

Oke, P. R., Griffin, D. A., Schiller, A., Matear, R. J., Fiedler, R., Mansbridge, J., Lenton, A., Cahill, M., Chamberlain, M. A., and Ridgway, K.: Evaluation of a near-global eddy-resolving ocean model, Geosci. Model Dev., 6, 591–615, doi:10.5194/gmd-6-591-2013, 2013.

Oschlies, A. and Schartau, M.: Basin-scale performance of a locally optimized marine ecosystem model, J. Marine Res., 63, 335–358, 2005.

Puri, K., Dietachmayer, G., Steinle, P., Dix, M., Rikus, L., Logan, L., Naughton, M., Tingwell, C., Xiao, Y., Barras, V., Bermous, I., Bowen, R., Deschamps, L., Franklin, C., Fraser, J., Glowacki, T., Harris, B., Lee, J., Le, T., Roff, G., Sulaiman, A., Sims, H., Sun, X., Sun, Z., Zhu, H., Chattopadhyay, M., and Engel, C.: Implementation of the initial ACCESS numerical weather prediction system, Aust. Meteor. Oceanogr. J., 63, 265–284, 2013.

Seferian, R., Gehlen, M., Bopp, L., Resplandy, L., Orr, J. C., Marti, O., Dunne, J. P., Christian, J. R., Doney, S. C., Ilyina, T., Lindsay, K., Halloran, P., Heinze, C., Segschneider, J., and Tjiputra, J.: Inconsistent strategies to spin up models in CMIP5: implications for ocean biogeochemical model performance assessment, Geoscientific Model Development Discussions, 8, 8751–8808, 2015.

Shao, P., Zeng, X., Sakaguchi, K., Monson, R. K., and Zeng, X.: Terrestrial carbon cycle: climate relations in eight CMIP5 Earth System Models, J. Climate, 26, 8744–8764, 2013.

Takahashi, T., Sutherland, S. C., Wanninkhof, R., Sweeney, C., Feely, R. A., Chipman, D. W., Hales, B., Friederich, G., Chavez, F., Sabine, C. L., Watson, A., Bakker, D. C. E., Schuster, U., Metzl, N., Yoshikawa-Inoue, H., Ishii, M., Midorikawa, T., Nojiri, Y., Koertzinger, A., Steinhoff, T., Hoppema, M., Olafsson, J., Arnarson, T. S., Tilbrook, B., Johannessen, T., Olsen, A., Bellerby, R., Wong, C. S., Delille, B., Bates, N. R., and Baar, H. J. W. d.: Climatological mean and decadal change in surface ocean pCO(2), and net sea-air CO2 flux over the global oceans, Deep Sea Research Part II: Topical Studies in Oceanography, 56, 554–577, 2009.

Taylor, K. E.: Summarizing multiple aspects of model performance in a single diagram, J. Geophys. Res., 106, 7183–7192, 2001.

Taylor, K. E., Stouffer, R. J., and Meehl, G. A.: An overview of CMIP5 and the experiment design, B. Am. Meteorol. Soc., 93, 485–498, doi:10.1175/BAMS-D-11-00094.1, 2012.

The HadGEM2 Development Team: G. M. Martin, Bellouin, N., Collins, W. J., Culverwell, I. D., Halloran, P. R., Hardiman, S. C., Hinton, T. J., Jones, C. D., McDonald, R. E., McLaren, A. J., O'Connor, F. M., Roberts, M. J., Rodriguez, J. M., Woodward, S., Best, M. J., Brooks, M. E., Brown, A. R., Butchart, N., Dearden, C., Derbyshire, S. H., Dharssi, I., Doutriaux-Boucher, M., Edwards, J. M., Falloon, P. D., Gedney, N., Gray, L. J., Hewitt, H. T., Hobson, M., Huddleston, M. R., Hughes, J., Ineson, S., Ingram, W. J., James, P. M., Johns, T. C., Johnson, C. E., Jones, A., Jones, C. P., Joshi, M. M., Keen, A. B., Liddicoat, S., Lock, A. P., Maidens, A. V., Manners, J. C., Milton, S. F., Rae, J. G. L., Ridley, J. K., Sellar, A., Senior, C. A., Totterdell, I. J., Verhoef, A., Vidale, P. L., and Wiltshire, A.: The HadGEM2 family of Met Office Unified Model climate configurations, Geosci. Model Dev., 4, 723–757, doi:10.5194/gmd-4-723-2011, 2011.

Trenberth, K. E., Dai, A., Rasmussen, R. M., and Parsons, D. B.: The changing character of precipitation, B. Am. Meteorol. Soc., 84, 1205–1217, 2003.

Uotila, P., O'Farrell, S., Marsland, S. J., and Bi, D.: The sea-ice performance of the Australian climate models participating in the CMIP5, Aust. Meteor. Oceanogr. J., 63, 121–143, 2013.

Valcke, S.: OASIS3 User Guide (prism 2–5), PRISM Support Initiative Report No 3, CERFACS, Toulouse, France, 2006.

Valcke, S.: The OASIS3 coupler: a European climate modelling community software, Geosci. Model Dev., 6, 373–388, doi:10.5194/gmd-6-373-2013, 2013.

Valcke, S., Craig, T., and Coquart, L.: OASIS3-MCT User Guide, OASIS3-MCT_2.0, CERFACS Technical Report TR-CMGC-13-17, CERFACS/CNRS SUC URA No 1875, Toulouse, France, available at: http://pantar.cerfacs.fr/globc/publication/technicalreport/2013/oasis3mct_UserGuide.pdf (last access: 16 September 2015), 2013.

Wang, Y. P. and Leuning, R.: A two-leaf model for canopy conductance, photosynthesis and partitioning of available energy I. Model description and comparison with a multi-layered model, Agr. Forest Meteorol., 91, 89–111, 1998.

Wang, Y. P., Law, R. M., and Pak, B.: A global model of carbon, nitrogen and phosphorus cycles for the terrestrial biosphere, Biogeosciences, 7, 2261–2282, doi:10.5194/bg-7-2261-2010, 2010.

Wang, Y. P., Kowalczyk, E., Leuning, R., Abramowitz, G., Raupach, M. R., Pak, B., van Gorsel, E., and Luhar, A.: Diagnosing errors in a land surface model (CABLE) in the time and frequency domains, J. Geophys. Res., 116, G01034, doi:10.1029/2010JG001385, 2011.

Wang, Y. P., Lu, X. J., Wright, I. J., Dai, Y. J., Rayner, P. J., and Reich, P. B.: Correlations among leaf traits provide a significant constraint on the estimate of global gross primary production, Geophys. Res. Lett., 39, L19405, doi:10.1029/2012GL053461, 2012.

Wang, Y. P., Zhang, Q., Pitman, A. J., and Dai, Y. J.: Nitrogen and phosphorus limitation reduces the effects of land use change on land carbon uptake and emission, Environ. Res. Lett., 10, 014001, doi:10.1088/1748-9326/10/014001, 2015.

Wanninkhof, R.: Relationship between wind speed and gas exchange over the ocean, J. Geophys. Res., 97, 7373–7382, doi:10.1029/92JC00188, 1992.

Wilson, D. R., Bushell, A. C., Kerr-Munslow, A. M., Price, J. D., and Morcrette, C. J.: PC2: a prognostic cloud fraction and condensation scheme, I: Scheme description, Q. J. Roy. Meteor. Soc., 134, 2093–2107, 2008.

Woodward, S.: Modeling the atmospheric life cycle and radiative impact of mineral dust in the Hadley Centre climate model, J. Geophys. Res., 106, 18155–18166, doi:10.1029/2000JD900795, 2001.

Woodward, S.: Mineral dust in HadGEM2, Hadley Centre Technical Note 87, Met Office Hadley Centre, Exeter, UK, available at: http://www.metoffice.gov.uk/media/pdf/l/p/HCTN_87.pdf (last access: 12 August 2015), 2011.

Zhang, Q., Wang, Y. P., Pitman, A. J., and Dai, Y. J.: Limitations of nitrogen and phosphorous on the terrestrial carbon uptake in the 20th century, Geophys. Res. Lett., 38, L22701, doi:10.1029/2011GL049244, 2011.

Zhang, Q., Pitman, A. J., Wang, Y. P., Dai, Y. J., and Lawrence, P. J.: The impact of nitrogen and phosphorous limitation on the estimated terrestrial carbon balance and warming of land use change over the last 156 yr, Earth Syst. Dynam., 4, 333–345, doi:10.5194/esd-4-333-2013, 2013.

Zhang, Q., Wang, Y. P., Matear, R. J., Pitman, A. J., and Dai, Y. J.: Nitrogen and phosphorous limitations significantly reduce future allowable CO_2 emissions, Geophys. Res. Lett., 41, 632–637, doi:10.1002/2013GL058352, 2014.

Zhang, X. Y., Friedl, M. A., Schaaf, C. B., and Strahler, A. H.: Climate controls on vegetation phenological patterns in northern mid- and high latitudes inferred from MODIS data, Glob. Change Biol., 10, 1133–1145, 2004.

Zhang, X. Y., Friedl, M. A., Schaaf, C. B., Strahler, A. H., and Liu, Z.: Monitoring the response of vegetation phenology to precipitation in Africa by coupling MODIS and TRMM instruments, J. Geophys. Res., 110, D12103, doi:10.1029/2004JD005263, 2005.

Ziehn, T., Lenton, A., Law, R. M., Matear, R. M., and Chamberlain, M.: The carbon cycle in the Australian Community Climate and Earth System Simulator (ACCESS-ESM1) – Part 2: Historical simulation, Geosci. Model Dev. Discuss, ~~in preparation, 2015.~~ submitted, 2016.

Table 1. Model Parameters of the BGC model were set to the values optimised in the 1-D model of the Southern Ocean (Oschlies and Schartau, 2005).

Parameter	Units	Value
Phytoplankton model parameters		
Initial slope of P-I curve	$day^{-1}\,(W\,m^{-2})^{-1}$	0.256
Photosynthetically active radiation	–	0.43
Maximum growth rate parameters	day^{-1}, –, C^{-1}	0.27, 1.066, 1.0
Half saturation constant for N uptake	$mmol\,N\,m^{-3}$	0.7
Half saturation constant for Fe uptake	$\mu mol\,Fe\,m^{-3}$	0.1
Phytoplankton mortality	day^{-1}	0.04 b^{cT}
Quadratic mortality	$(mmol\,N\,m^{-3})^{-1}\,day^{-1}$	0.25
Zooplankton model parameters		
Assimilation efficiency	–	0.925
Maximum grazing rate	day^{-1}	1.575
Prey capture rate	$(mmol\,N\,m^{-2})^{-1}\,day^{-1}$	1.6
Quadratic mortality	$(mmol\,N\,m^{-3})^{-1}\,day^{-1}$	0.34
Excretion	day^{-1}	0.01 b^{cT}
Detritus model parameters		
Remineralisation rate ($< 180\,m$)	day^{-1}	0.048 b^{cT}
Remineralisation rate ($\geq 180\,m$)	day^{-1}	0.024 b^{cT}
Sinking velocity	$m\,day^{-1}$	18.0
$CaCO_3$ model parameters		
Remineralisation rate	day^{-1}	0.0035
Sinking velocity	$m\,day^{-1}$	10.0
Inorganic fraction	–	0.08
Fe model parameters		
Scavenging rate	day^{-1}	0.00274
Background	$\mu mol\,Fe\,m^{-3}$	0.1

Table 2. Standard deviation of annual global carbon flux for years 901–1000 in $\mathrm{Pg\,C\,yr^{-1}}$.

	PresLAI	ProgLAI
GPP	1.17	1.87
Leaf resp	0.26	0.75
Plant resp	0.17	0.27
Soil resp	0.27	0.32
NEE	1.40	1.21

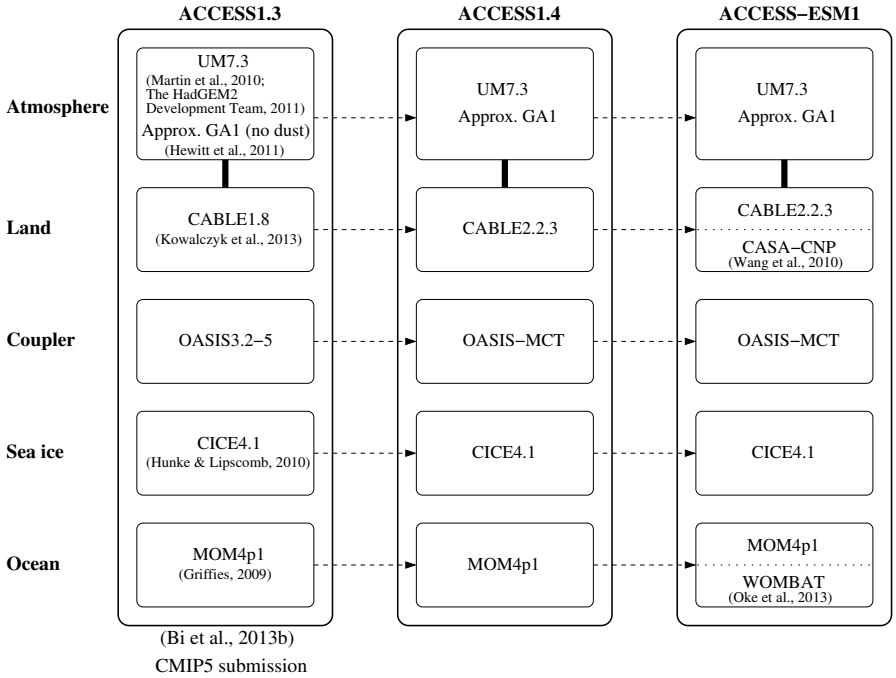

Figure 1. Schematic showing the different component models of ACCESS-ESM1 and the ACCESS versions on which it is dependent.

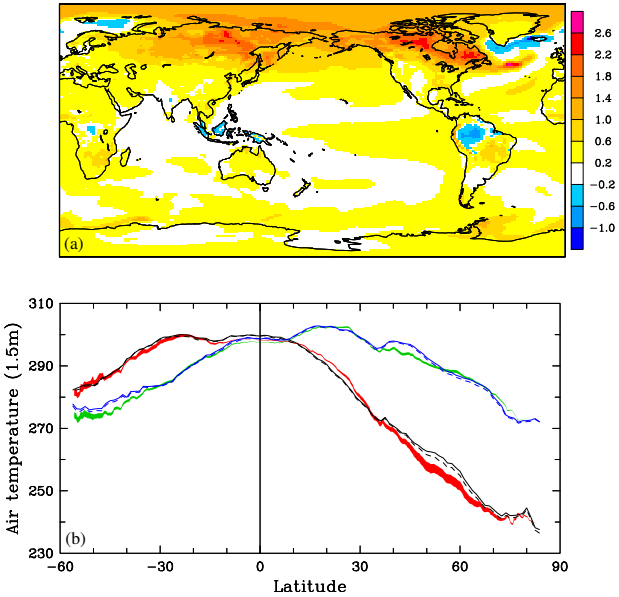

Figure 2. ~~Root mean square~~ Surface air temperature difference ~~(RMSD)~~ **(a)** between ~~atmospheric variables simulated by the model versions listed in the key~~ ProgLAI and ~~those from the ACCESS1.3 pre-industrial simulation normalised by the RMSD between ACCESS1.0~~ PresLAI for years 901-1000 and ~~ACCESS1.3. The variables are precipitation (pr),~~ zonal mean land surface air temperature **(b)** for ProgLAI in January (~~tas~~)black, ~~sea level pressure (psl~~solid) ~~, top of atmosphere long-wave radiation and July (rlut~~)blue, ~~top of atmosphere reflected short-wave radiation (rsut~~solid) ~~, air temperature~~ and for PresLAI in January (~~ta~~)black, ~~zonal (ua~~dashed) and ~~meridional wind~~ July (~~va~~blue, dashed)~~at 850~~ . The zonal mean ± one standard deviation 1901-1910 observed land surface air temperature (Jones and Harris, 2014) is shown by the red shaded region for January and ~~200 and geopotential height (zg) at 500~~ the green shaded region for July.

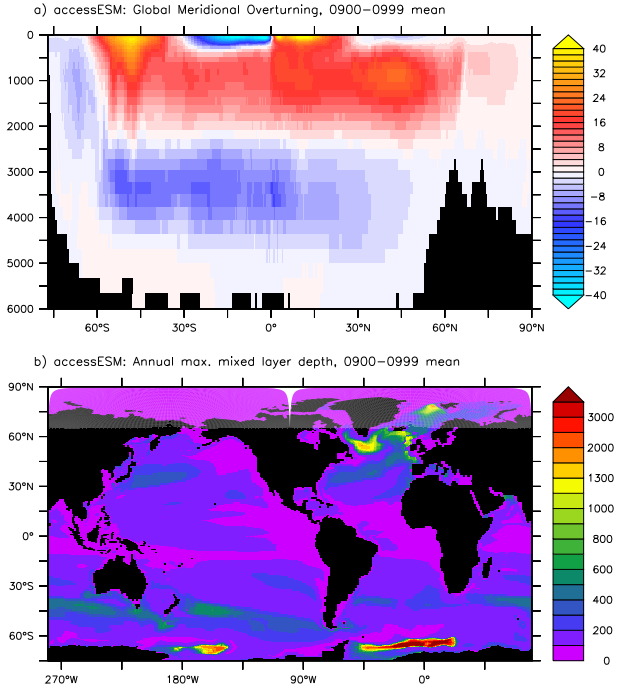

Figure 3. ~~Global Meridional Overturning Streamfunction (Sv)~~ ACCESS-ESM1 from the last 100 year average of the pre-industrial simulation for **(a)** ~~ACCESS1.3~~ Global Meridional Overturning Streamfunction (Sv) and **(b)** ~~ACCESS1.4 pre-industrial simulations~~maximum annual mixed layer depth (m).

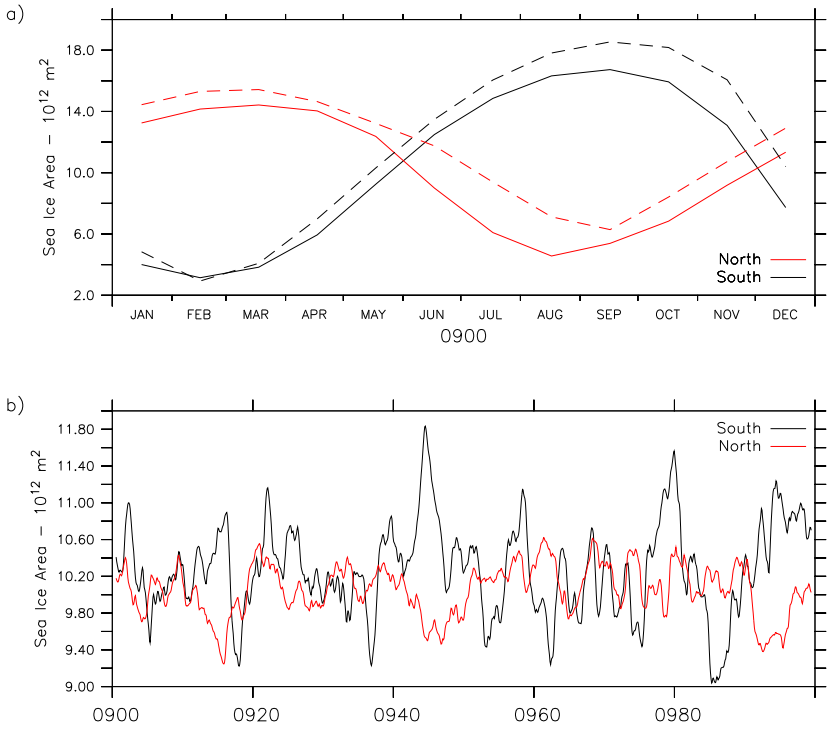

Figure 4. ~~Maximum mixed layer~~ ACCESS-ESM 1 simulated (~~m~~solid) and observed (dashed) sea-ice area for the northern and southern hemisphere from the last 100 year ~~average~~ of the pre-industrial simulation for **(a)** ~~ACCESS1.3 and~~ seasonal climatology **(b)** ~~ACCESS1.4 pre-industrial simulations~~annual mean area. The observed sea icea observations are based on Comiso (2000)

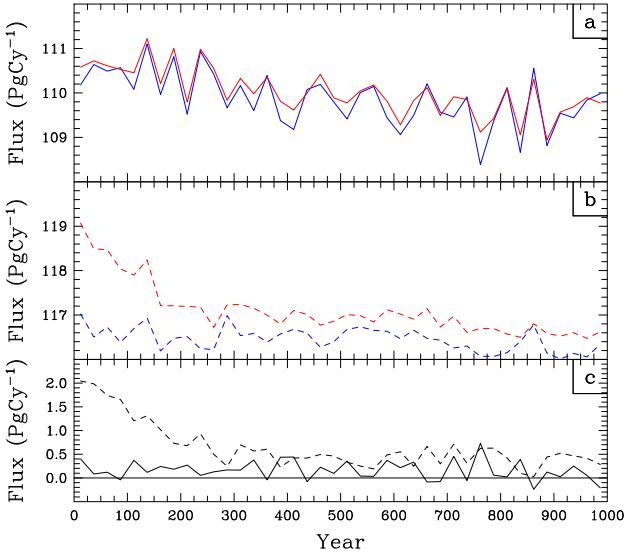

Figure 5. 25 year mean global GPP (blue) and summed respiration (red) in Pg C yr^{-1} for the ProgLAI simulation **(a)** and the PresLAI simulation **(b)**. Panel **(c)** shows 25 year mean global NEE in Pg C yr^{-1} for ProgLAI (solid) and PresLAI (dashed).

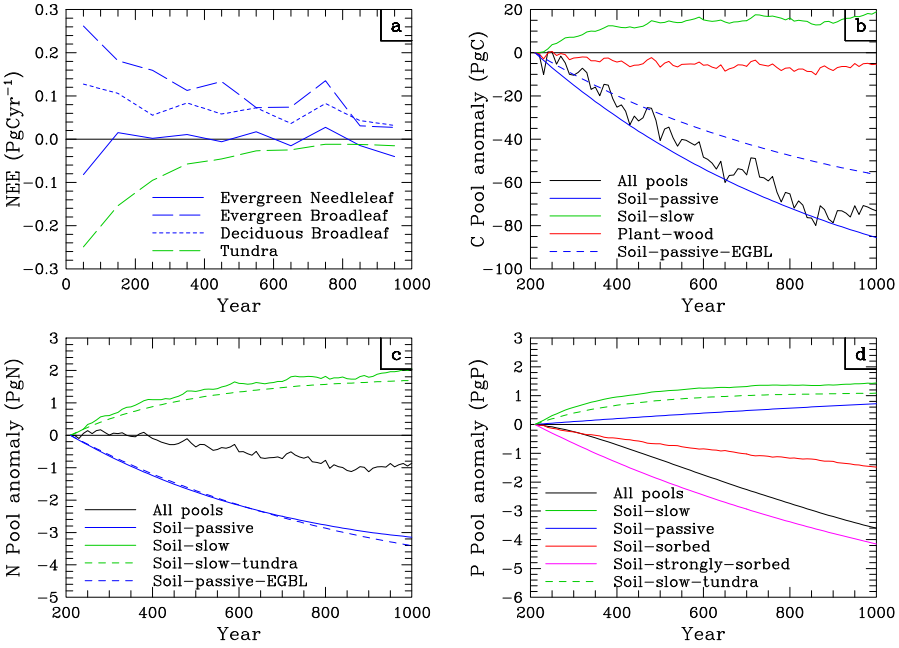

Figure 6. 100 year mean global NEE **(a)** in Pg C yr^{-1} for selected vegetation types as listed in the key and carbon ~~pool size~~ **(b)**, nitrogen **(c)** and phosphorus **(d)** pool sizes in Pg C, Pg N and Pg P at the end of each 10 years relative to year 210 for the sum of all ~~carbon~~ pools (black), and selected ~~carbon~~ pools (~~passive soil, blue solid~~as listed in the key; ~~slow soil~~solid: pools summed over vegetation type, ~~green; plant wood, red and passive soil~~ dashed: pools for listed vegetation type, EGBL=evergreen broadleaf~~trees, blue dash~~) for the ProgLAI simulation. The horizontal black line indicates zero NEE **(a)** and zero ~~C~~ pool anomaly ~~**(b)**~~**(b-d)**.

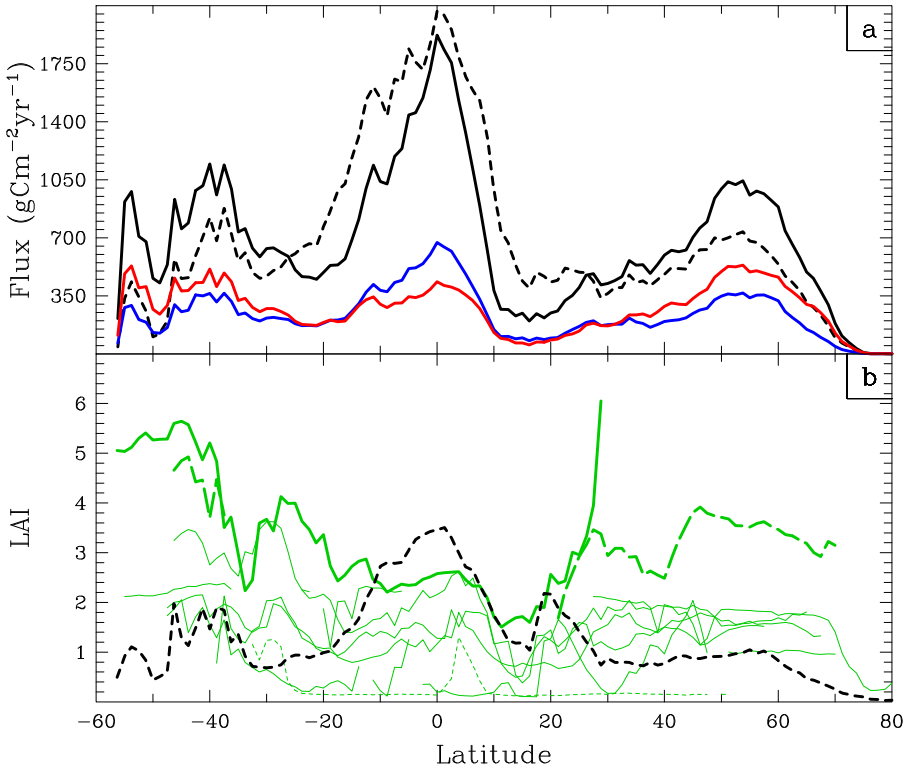

Figure 7. Zonal mean year 501–1000 carbon flux **(a)** in g C m^{-2}yr^{-1} and leaf area index **(b)**. Carbon fluxes are zonally averaged over all land grid-cells, showing from ProgLAI, GPP (black solid), plant respiration (blue) and soil respiration (red) and from PresLAI, GPP (black, dashed). For ProgLAI the LAI is zonally averaged over all tiles for each vegetation type separately (evergreen broadleaf trees, bold green; evergreen needleleaf trees, bold dashed green; C4 grass, dotted green; all other types, solid green). For PresLAI, the LAI is zonally averaged over all land grid-cells (black, dash).

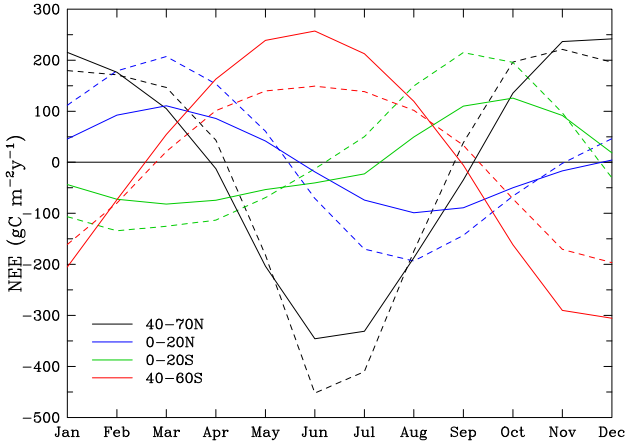

Figure 8. Monthly mean NEE in g C m^{-2}yr^{-1} for years 901–1000 averaged over the land grid-cells in four latitude bands (as listed in the key), for PresLAI (dashed) and ProgLAI (solid).

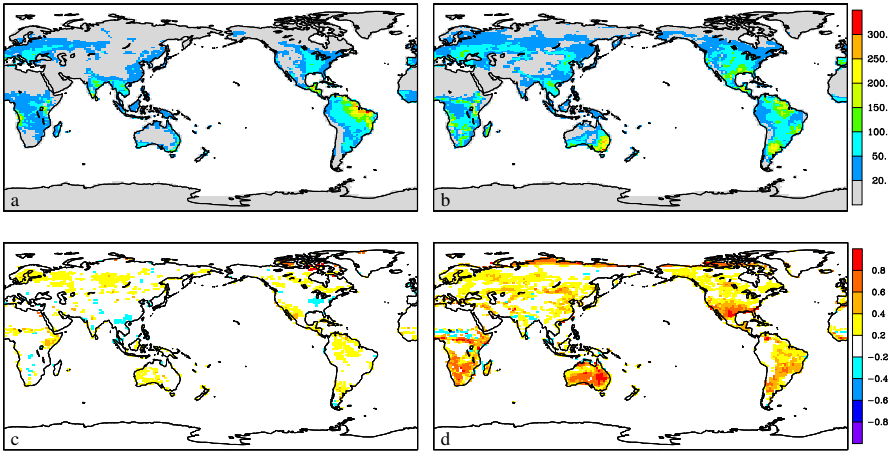

Figure 9. Standard deviation of annual NEE **(a, b)** in $\mathrm{g\,C\,m^{-2}yr^{-1}}$ for years 901–1000 and the autocorrelation for NEE with one year lag **(c, d)** for PresLAI (left) and ProgLAI (right).

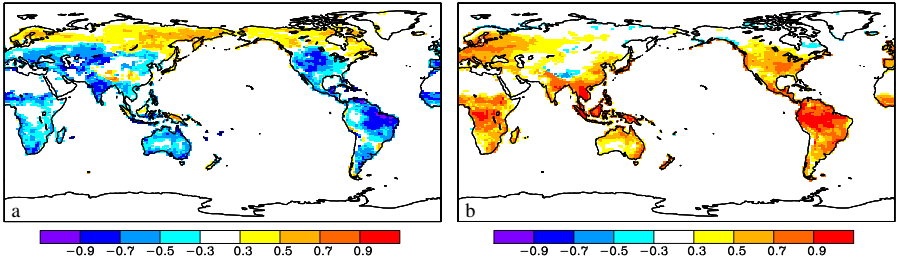

Figure 10. Correlation between annual NEE and **(a)** annual mean precipitation and **(b)** annual mean screen-level temperature for years 901–1000 from the ProgLAI simulation.

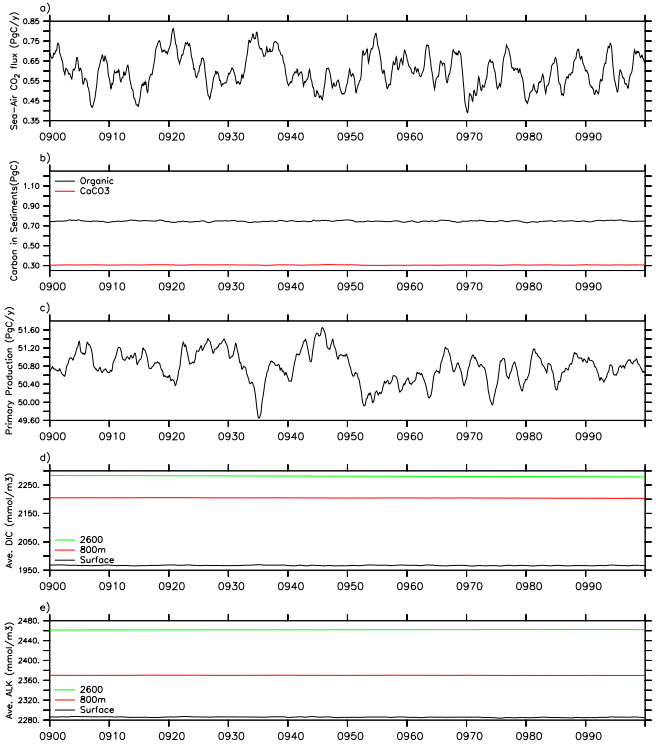

Figure 11. ~~Global~~ For the ACCESS-ESM1 simulation the global **(a)** sea–air flux of carbon dioxide $\mathrm{Pg\,C\,yr^{-1}}$, **(b)** carbon content of the organic (black) and calcium carbon sediment (red) pools in Pg C, ~~and~~ **(c)** net primary productivity in $\mathrm{Pg\,C\,yr^{-1}}$, **(d)** global averaged dissolved inorganic carbon $\mathrm{mmol\,m^{-3}}$ at various depths, and **(e)** global average alkalinity $\mathrm{mmol\,m^{-3}}$ at various depths.

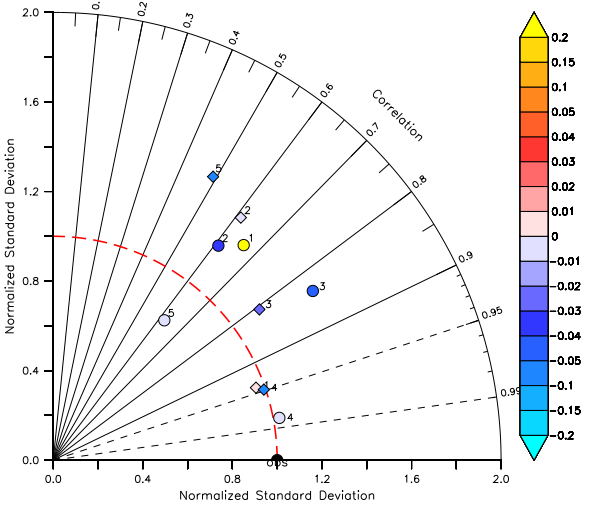

Figure 12. Taylor diagram assessing the response of the ACCESS-ESM1 simulations (circles), and the median of CMIP5 models (diamonds) with observations. The numbers correspond to: (1) ~~Nitrate~~Phosphate, (2) Alkalinity, (3) DIC, (4) SST, and (5) (sea surface) Salinity. For explanation of how to intepret the diagram please see the text.

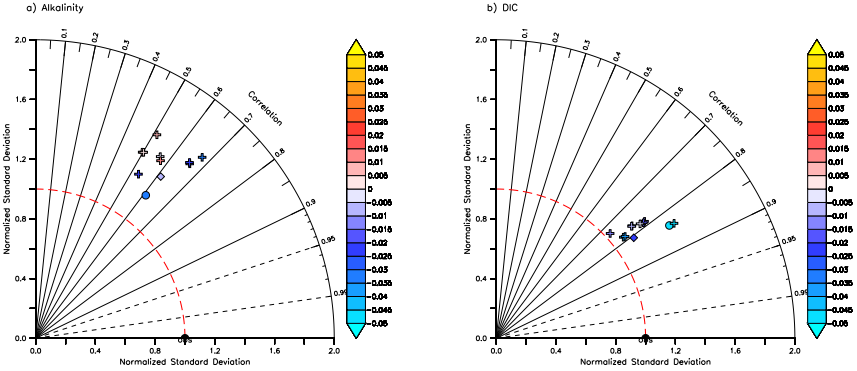

Figure 13. Taylor diagram assessing the ~~DIC~~ alkalinity **(a)** and ~~alkalinity~~ DIC **(b)** of the ACCESS-ESM1 simulation (circle), the median of CMIP5 models (diamond), and the individual members of the CMIP5 ensemble (crosses) with observations.

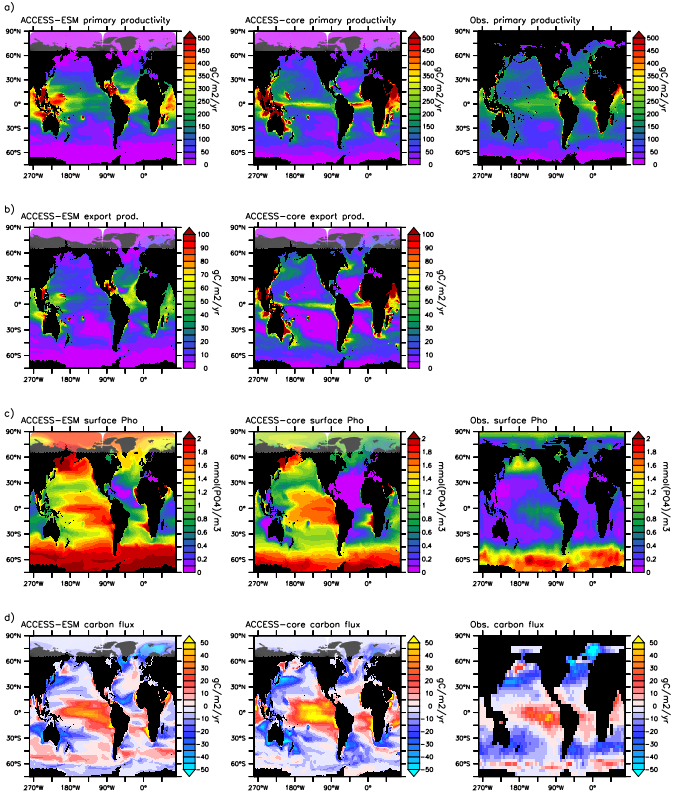
a)
ACCESS−ESM primary productivity
ACCESS−core primary productivity
Obs. primary productivity
gC/m2/yr
b)
ACCESS−ESM export prod.
ACCESS−core export prod.
gC/m2/yr
c)
ACCESS−ESM surface Pho
ACCESS−core surface Pho
Obs. surface Pho
mmol(PO4)/m3
d)
ACCESS−ESM carbon flux
ACCESS−core carbon flux
Obs. carbon flux
gC/m2/yr
90°N
60°N
30°N
0°
30°S
60°S
270°W
180°W
90°W
0°

Figure 14. ~~The mean sea–air flux~~ Comparison of ~~carbon dioxide~~ the ACCESS-ESM1 simulation (left column) for the years 901–1000 ~~(a)~~ with an ocean only simulation (middle column) and with the ~~interannual variability of~~ observations (right column) for **(a)** Primary productivity in $\mathrm{g\,C\,m^{-2}\,yr^{-1}}$, **(b)** Export production at 100 m in $\mathrm{g\,C\,m^{-2}\,yr^{-1}}$, **(c)** surface phosphate in $\mathrm{mmol P m^{-3}}$, and **(d)** mean sea–air flux of ~~defined as the standard deviation of annual fluxes for the years 901–1000~~ ~~(b)~~ carbon dioxide in $\mathrm{g\,C\,m^{-2}\,yr^{-1}}$. Observed primary productivity is based on the Eppley-VGPM algorithm. The surface phosphate observations come from the World Ocean Atlas climatology (WOA2005; Garcia et al., 2006a). The annual sea-air CO_2 fluxes are from Takahashi et al. (2009)

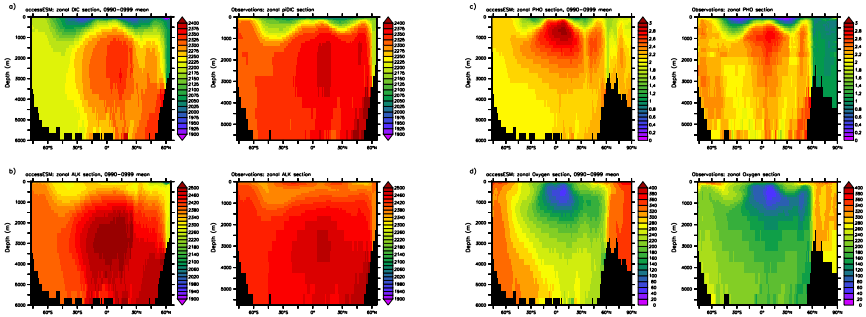

Figure 15. Zonal averaged sections of ACCESS-ESM1 simulation for the years 901–1000 (left) compared to the observations (right) for **(a)** DIC in mmolPm^{-3}, **(b)** Alkalinity in $\mathrm{mmolEqm}^{-3}$, **(c)** Phosphate in mmolPm^{-3}, and **(d)** Oxygen in mmolOm^{-3}

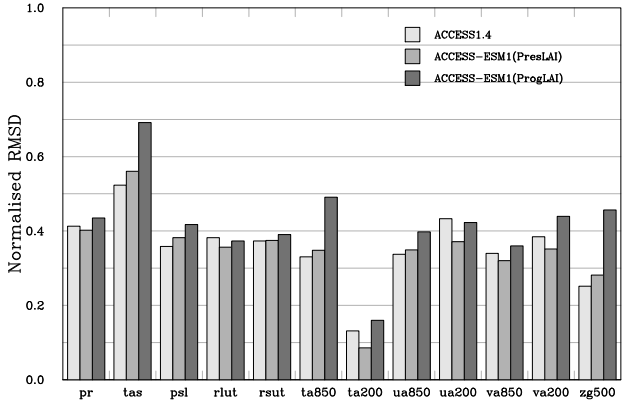

Figure 16. Root mean square difference (RMSD) between atmospheric variables simulated by the model versions listed in the key and those from the ACCESS1.3 pre-industrial simulation normalised by the RMSD between ACCESS1.0 and ACCESS1.3. The variables are precipitation (pr), surface air temperature (tas), sea level pressure (psl), top of atmosphere long-wave radiation (rlut), top of atmosphere reflected short-wave radiation (rsut), air temperature (ta), zonal (ua) and meridional wind (va) at 850 and 200 hPa and geopotential height (zg) at 500 hPa.